Bad Metallic Transport in a Cold Atom Fermi-Hubbard System

Peter Schauss
Stockholm, Nordita,
3.September 2018

PRINCETON UNIVERSITY

Bakr group, Princeton
Now: University of Virginia

Brown et. al., arXiv:1802.09456 (2018)

How can we understand quantum matter?

Strongly correlated materials

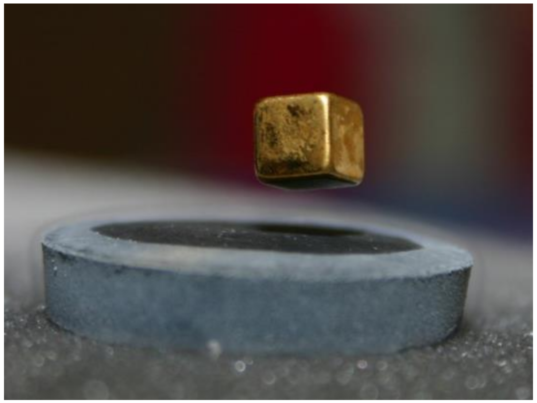

High T_c superconductors

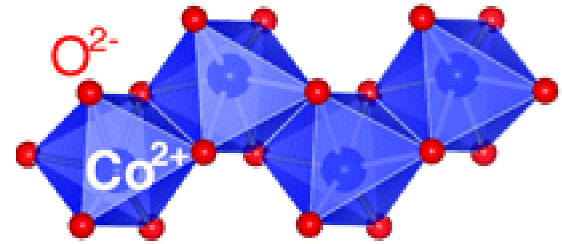

Quantum magnets

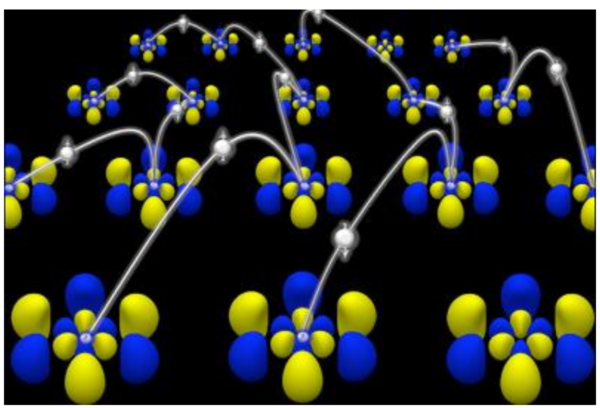

Heavy fermion metals

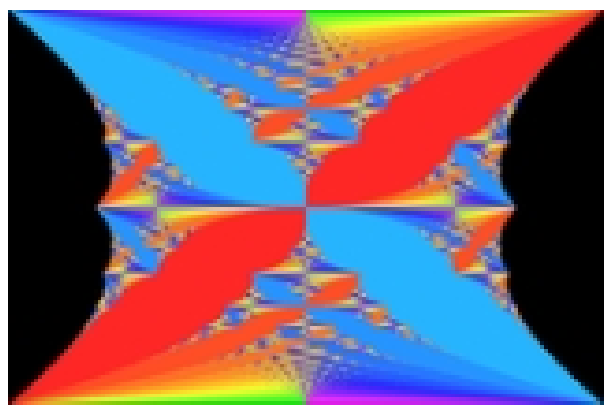

Topological phases

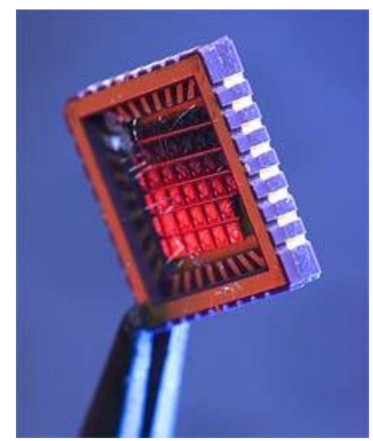

Spintronic materials

How can we understand quantum matter?

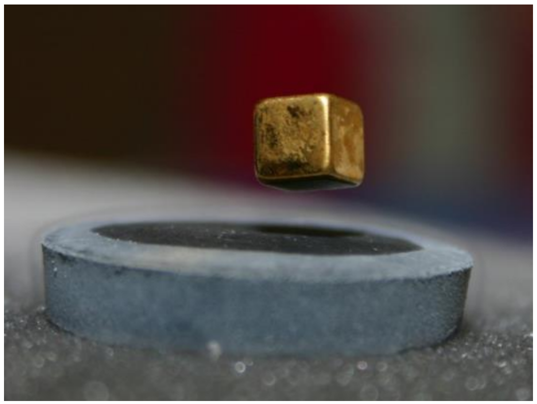

High T_c superconductors

Strongly correlated materials

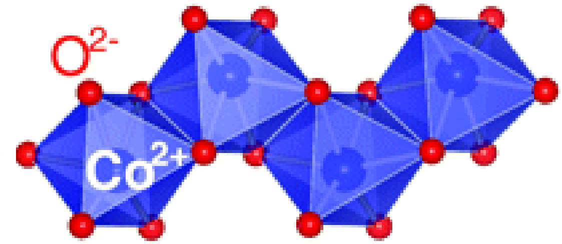

Quantum magnets

Condensed matter models

Hubbard model

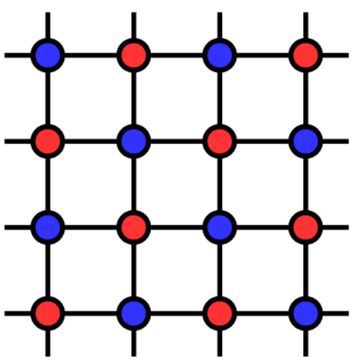

Quantum spin models (e.g. transverse Ising)

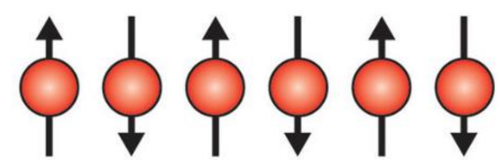

Interacting systems of ultracold atoms – enlarged model for condensed matter physics

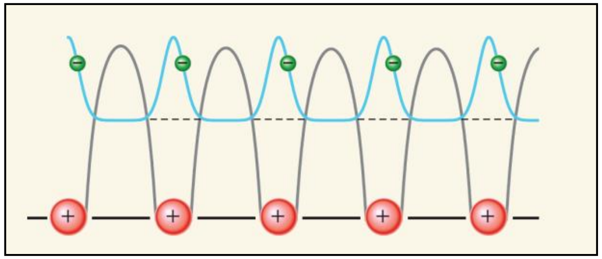

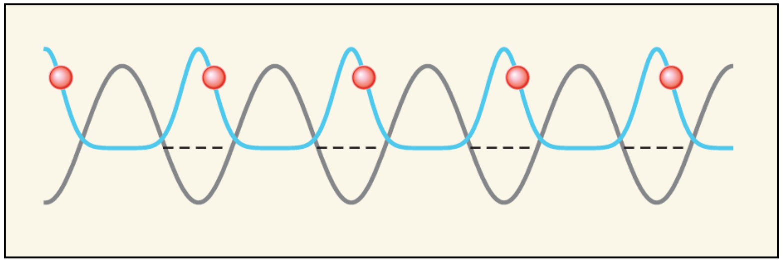

Why ultracold atoms?

- Complete control of microscopic parameters
- Clean systems, no lattice impurities
- Dynamics on observable timescales
- Understood from first principles
- Large interparticle spacing makes optical imaging/manipulation possible

Equilibrium vs. dynamics

Exact numerical techniques well-developed for equilibrium systems (QMC, NLCE, DMRG, etc.)

State of the art cold-atom Fermi-Hubbard experiments are just beyond reach of exact numerics.

Dynamics is much harder, especially for more than one dimension.

- Generalization of MPS to higher dimensions (PEPS) still needs more development.
- Cold atom experiments can provide benchmarks for testing algorithms.

Outline

1. Quantum gas microscopy
2. Antiferromagnetic correlations in the repulsive Hubbard model
3. Bad metallic transport in a cold atom Fermi-Hubbard system

Quantum gas microscopy

- Boson microscopes

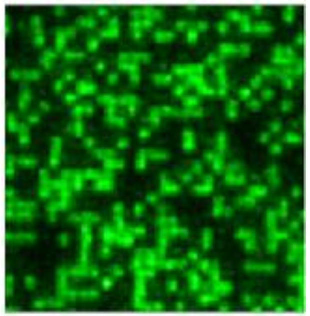

Harvard

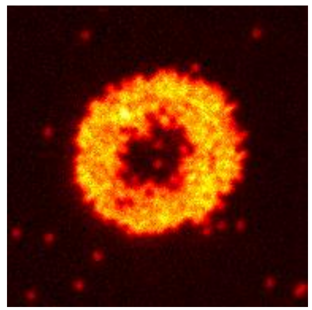

MPQ

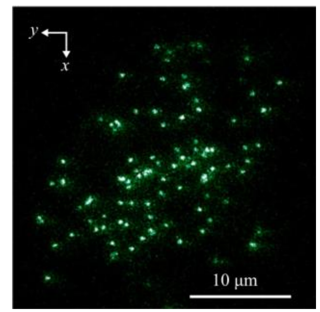

Kyoto

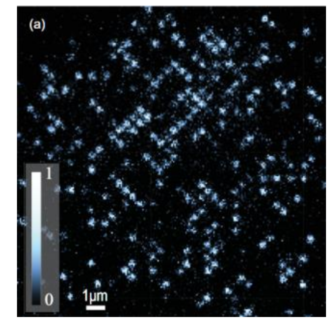

Tokyo

- Fermion microscopes

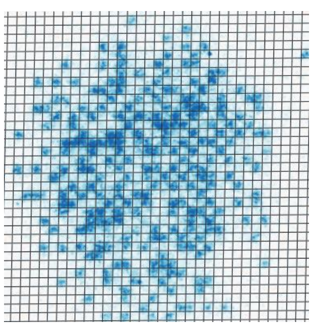

Harvard

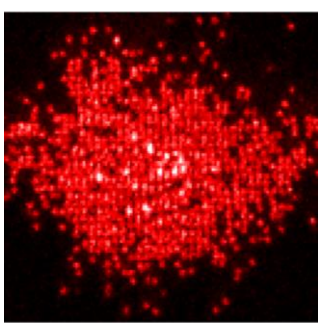

MPQ

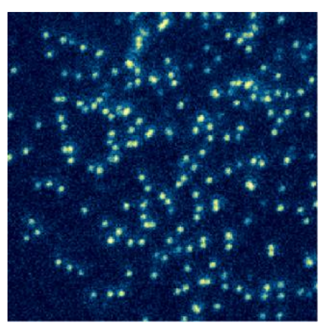

Strathclyde

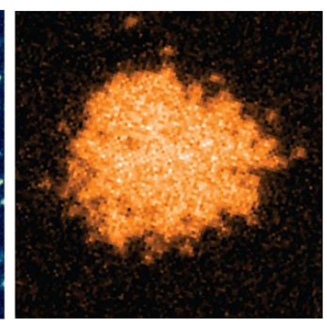

MIT

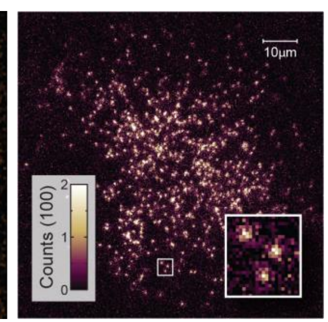

Toronto

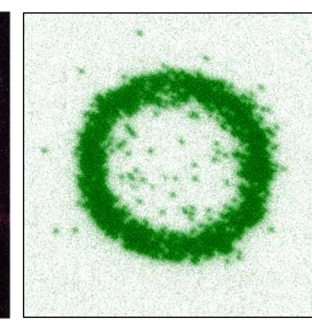

Princeton

The Fermi-Hubbard model

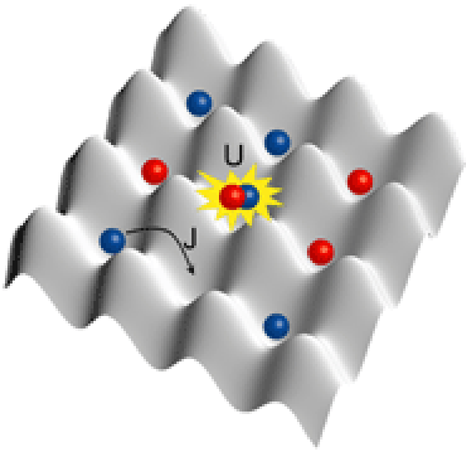

$$\mathcal{H} = -t \sum_{\langle ij \rangle, \sigma} \left(c^\dagger_{i,\sigma} c_{j,\sigma} + c^\dagger_{j,\sigma} c_{i,\sigma} \right) + U \sum_i n_{i,\uparrow} n_{i,\downarrow}$$

Realized naturally with cold atoms in optical lattices with fully tunable parameters.

Potentially rich phase diagram:

commensurate/incommensurate AFM, pseudogap, strange metal, d-wave superconductivity…

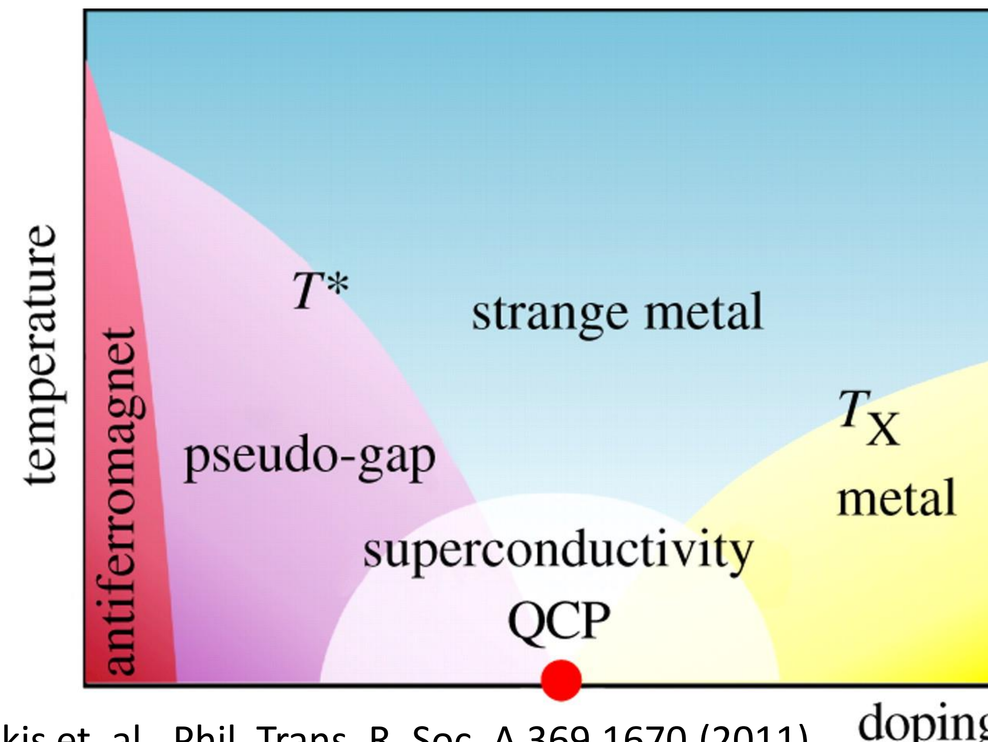

Galanakis et. al., Phil. Trans. R. Soc. A 369 1670 (2011)

A simplified Fermi gas microscope

- Single beam optical lattice @ 1064 nm simplifies microscopy:
  4-fold interference enhances depth + larger lattice spacing.

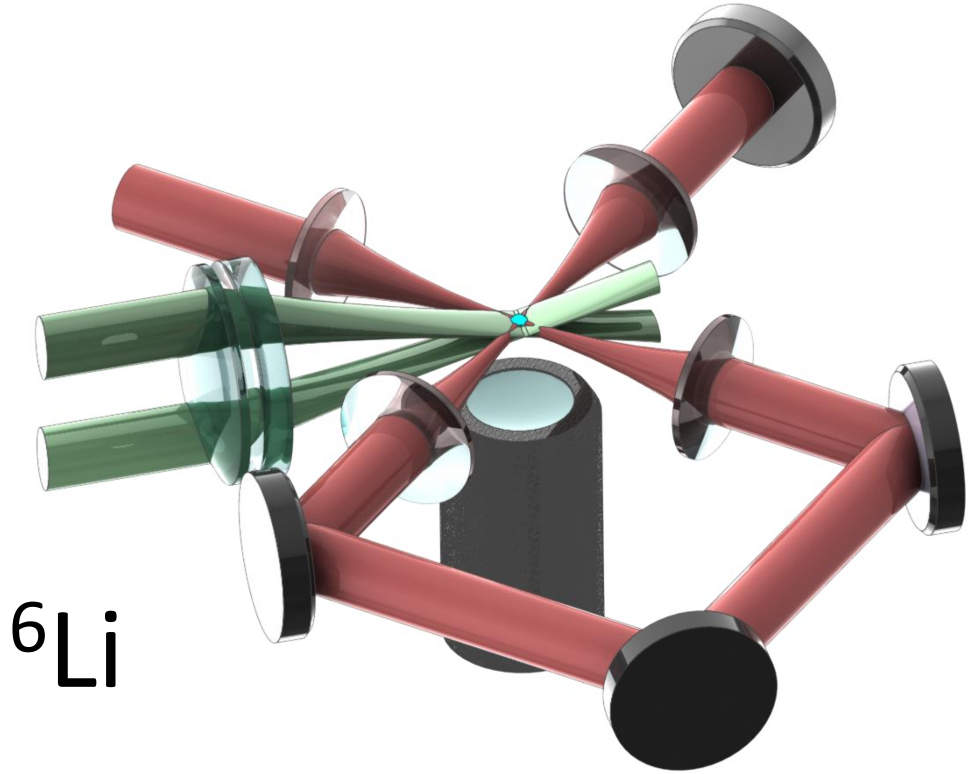

Vertical polarization: 752 nm

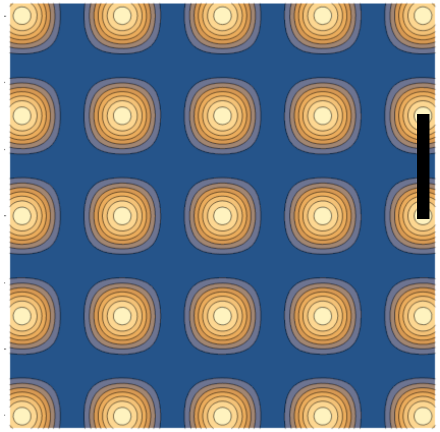

Horizontal polarization: 532 nm

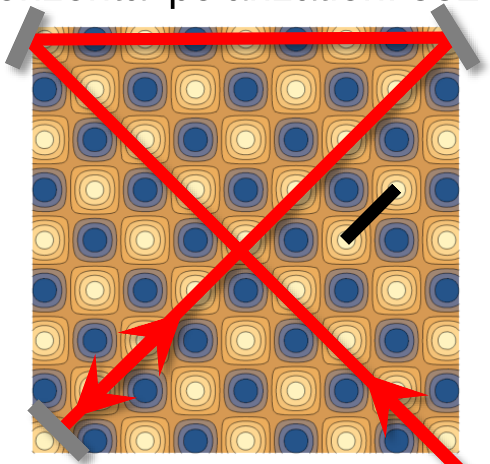

Lithium allows for large lattice spacing:

- Light
- "good" Feshbach resonances
- NA = 0.5 is sufficient for single-site resolution

Raman sideband cooling

- Raman cooling via D1 for fluorescence imaging

  In-plane lattice frequency: 1.5 MHz

  Axial confinement: 0.1 MHz

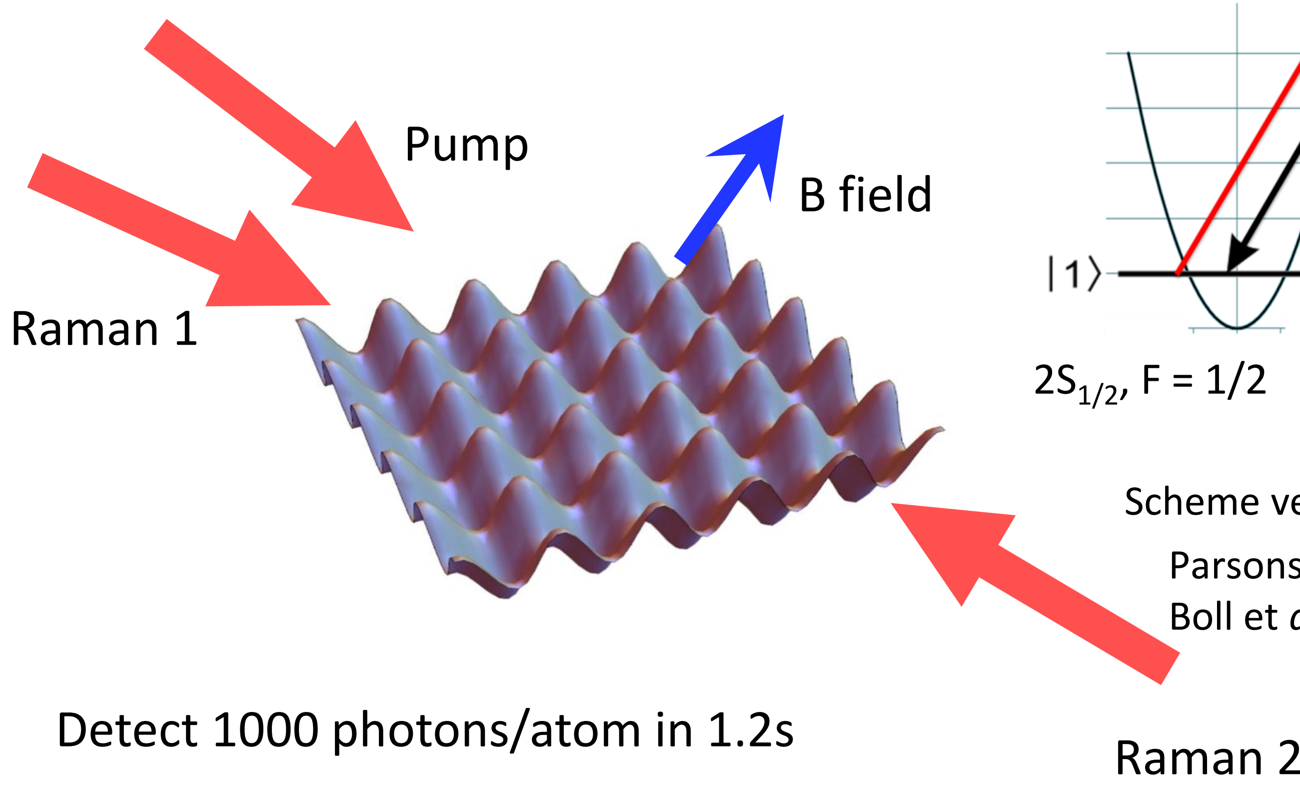

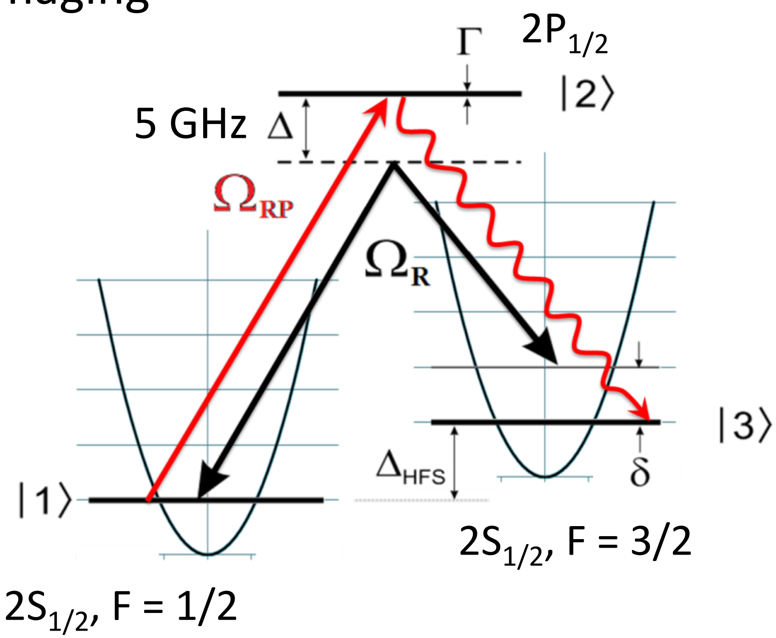

Detect 1000 photons/atom in 1.2s

Scheme very similar to:

Parsons et *al.*, Science **353**, 1253 (2016)
Boll et *al.*, Science **353**, 1257 (2016)

Image Reconstruction

- Hopping and loss from ~ 40 consecutive shots
- Hopping $=$ $0.4(2)\%$
- Loss $=$ $1.6(3)\%$

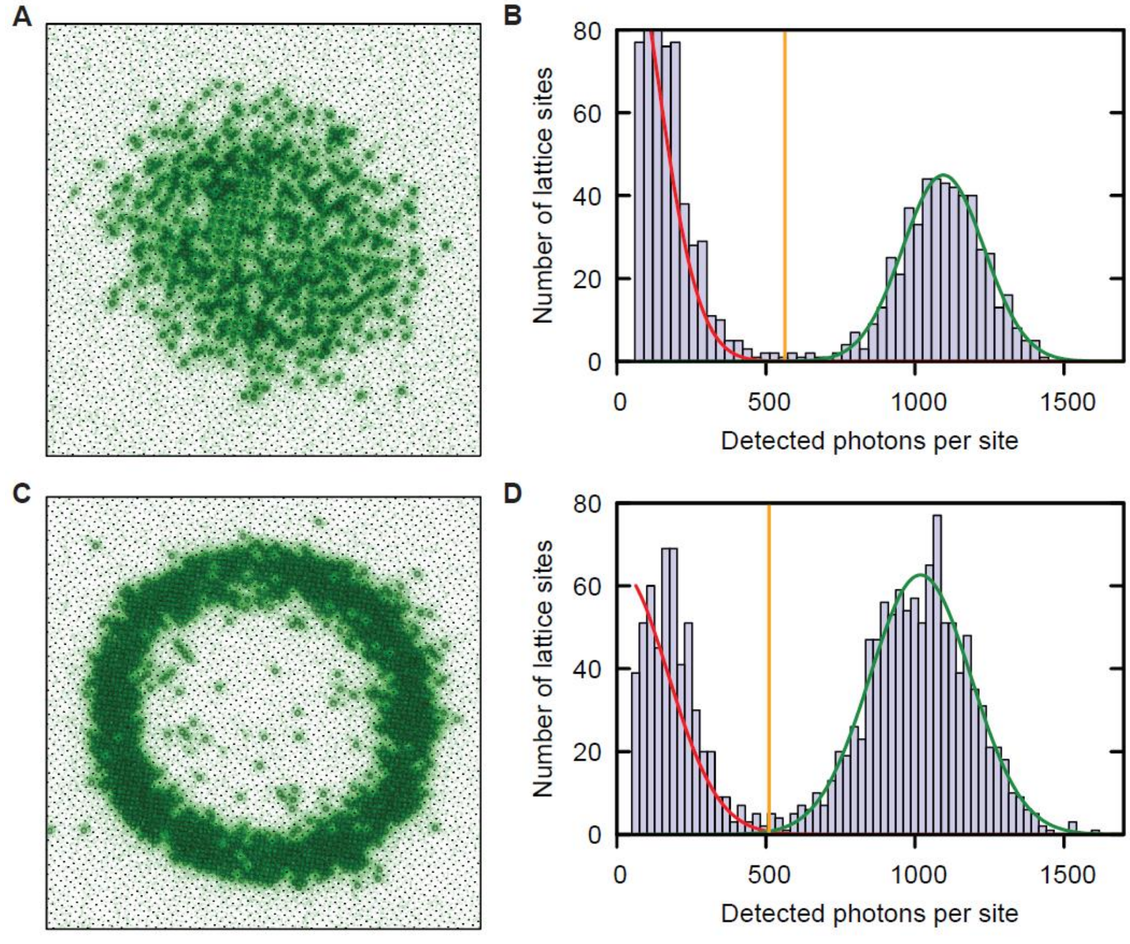

Reconstruction method: Nature **467**, 68 (2010)

Brown et. al., Science **357**, 1385 (2017)

2. Antiferromagnetic correlations in the repulsive Hubbard model

Brown et. al. Science **357**, 1385 (2017)

Antiferromagnetic correlations

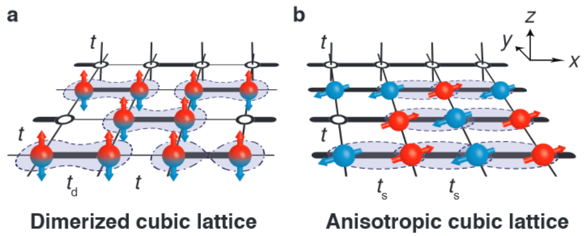

Esslinger group
Science 340, 1307 (2013)

Greiner group
T/t = 0.45 (2D)
Science 353, 1253 (2016)

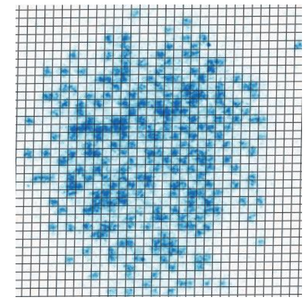

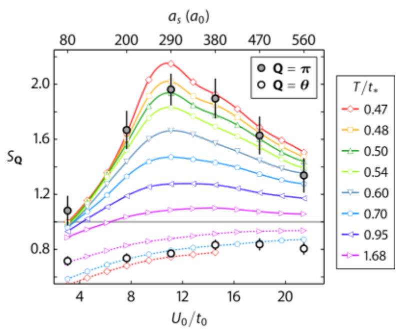

Hulet group
Nature 519, 211 (2015)

Bloch/Gross group
1D
Science 353, 1257 (2016)

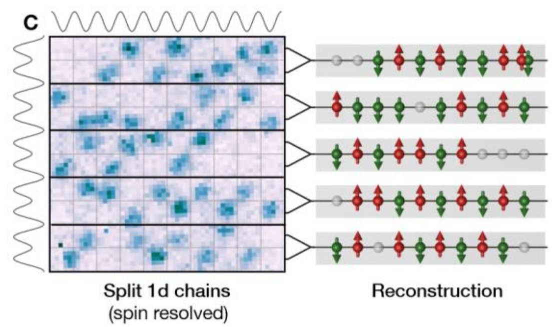

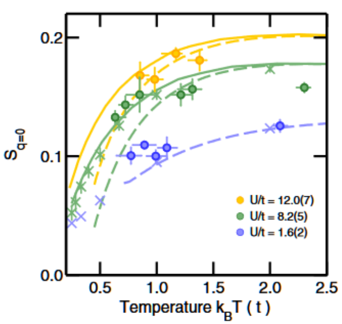

Köhl group (2D)
PRL 118, 170401 (2017)

Zwierlein group
T/t = 0.89 (2D)
Science 353, 1260 (2016)

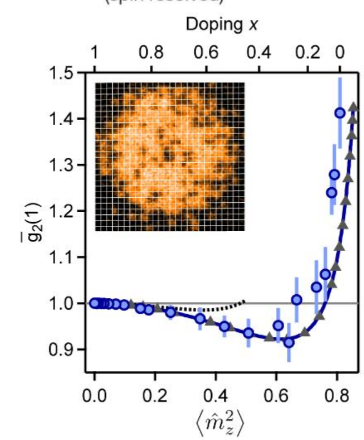

Spin imbalance

Condensed matter system:
Spin imbalance by applied magnetic field (Zeeman effect)

Cold atoms:

Spin-imbalance prepared before loading to lattice by evaporation in spin-dependent potential.

No spin-relaxation.

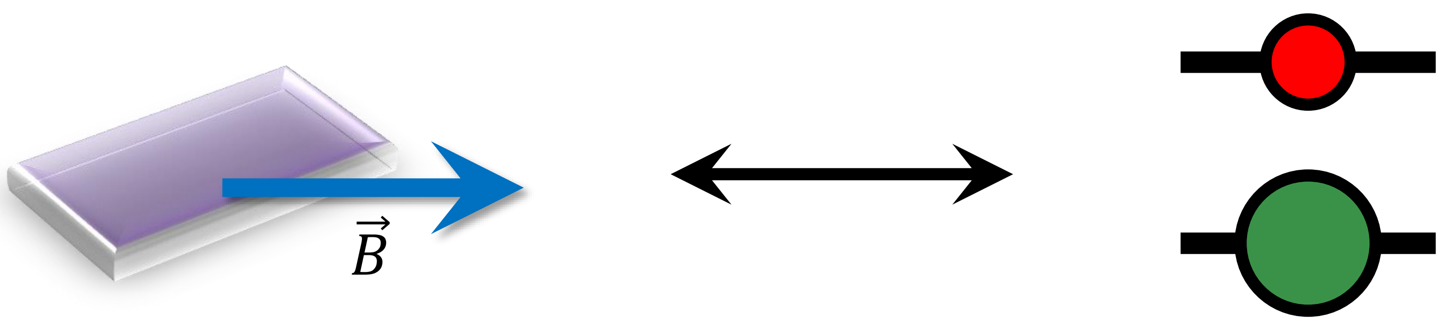

Zeeman field

Spin-polarization

Observables

- Density $\langle n_s \rangle, \langle n_\uparrow \rangle, \langle n_\downarrow \rangle, \langle n \rangle$
- Density of doublons $\langle n_d \rangle = \langle n_\uparrow n_\downarrow \rangle$
- Two-point correlators
  e.g. $C_\uparrow = \langle n_{\uparrow,i} n_{\uparrow j} \rangle - \langle n_{\uparrow,i} \rangle \langle n_{\uparrow,j} \rangle$
- Or: spin-spin correlators

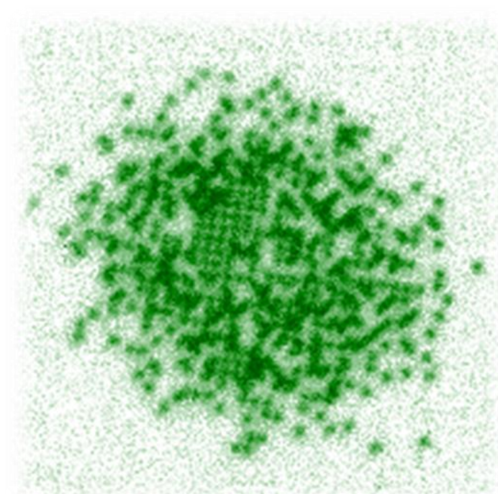

Brown et. al. Science **357**, 1385 (2017)

Probing spin-imbalanced lattice gases

- 1-3 mixture of lithium
- Evaporate in gradient
- Load into lattice at $U/t = 8$

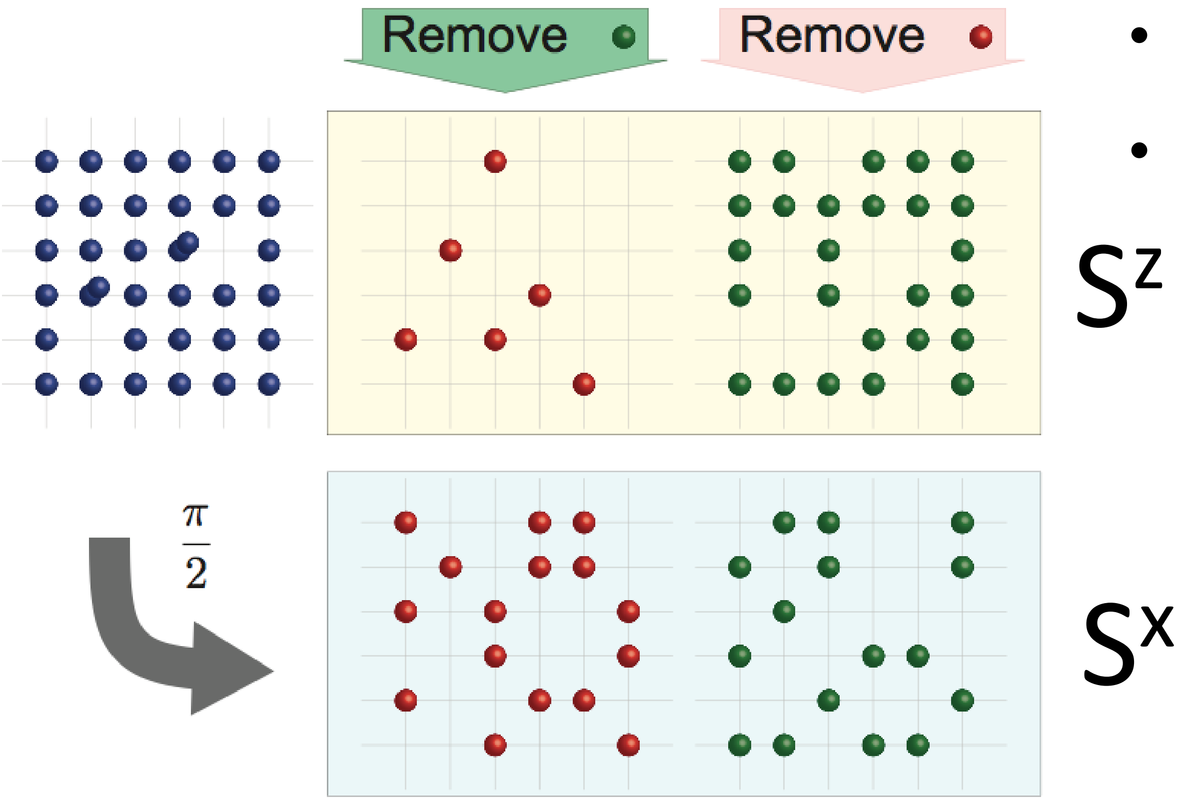

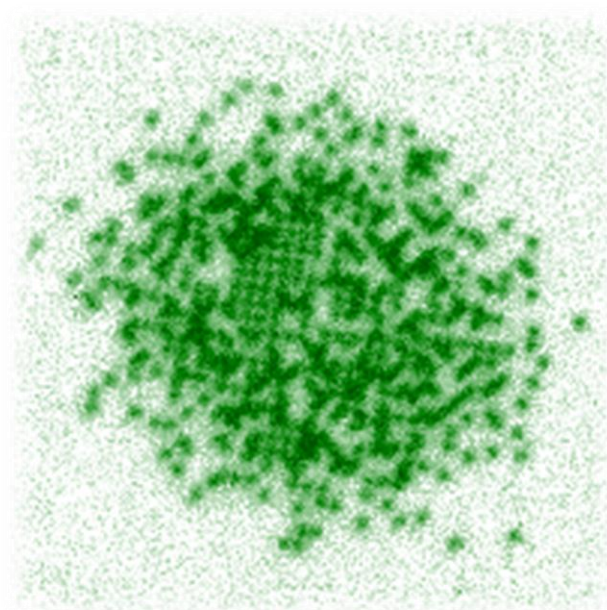

Vary: $$p^s = (n^s_\uparrow - n^s_\downarrow)/(n^s_\uparrow + n^s_\downarrow)$$

Brown et. al. Science **357**, 1385 (2017)

Anisotropic spin correlations

$$C^\alpha(\mathbf{d}) = 4\left(\langle S^\alpha_{\mathbf{i}} S^\alpha_{\mathbf{i+d}}\rangle - \langle S^\alpha_{\mathbf{i}}\rangle\langle S^\alpha_{\mathbf{i+d}}\rangle\right) \quad \alpha = z, \perp$$

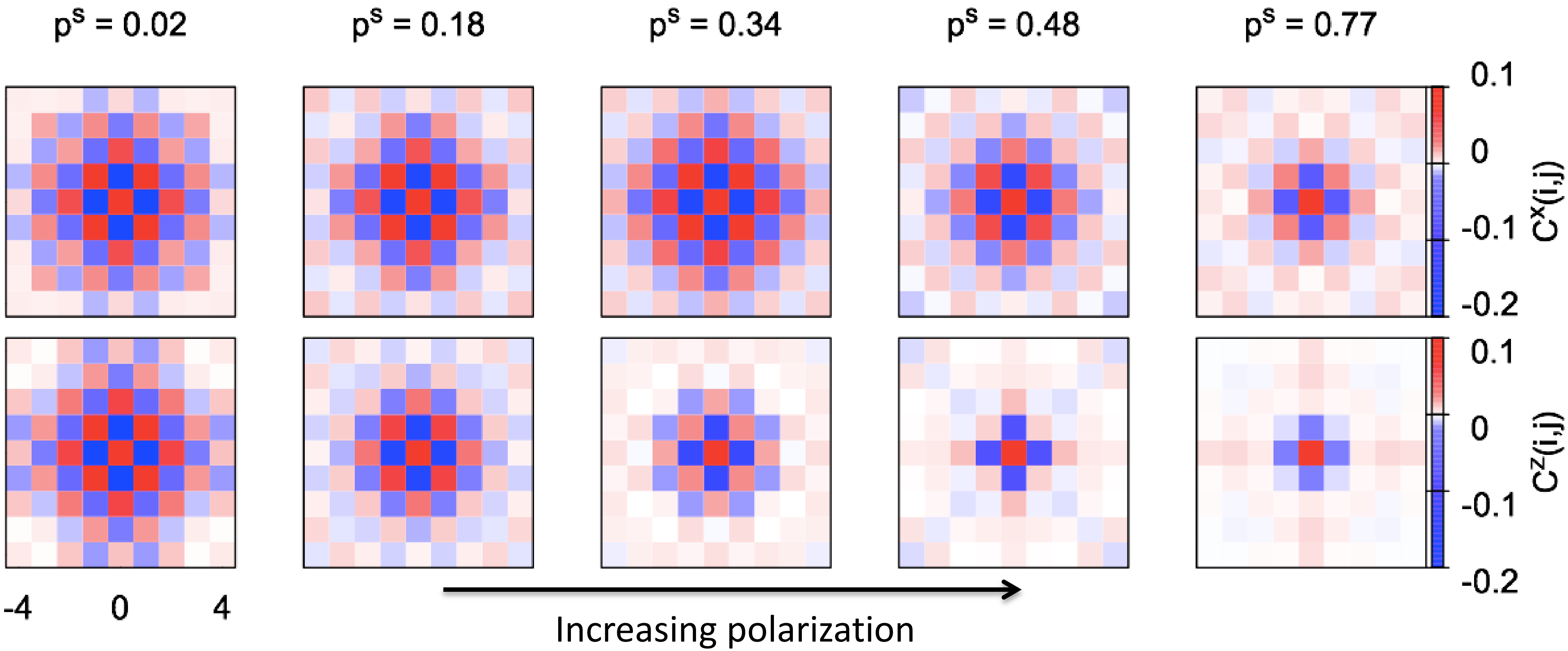

Unpolarized gas: isotropic spin correlations [SU(2) symmetry]

Polarized gas: AFM correlations preferred in the plane

3. Bad metallic transport in a cold atom Fermi-Hubbard system

Brown et. al, submitted, arXiv:1802.09456

Transport in ultracold Fermi gases

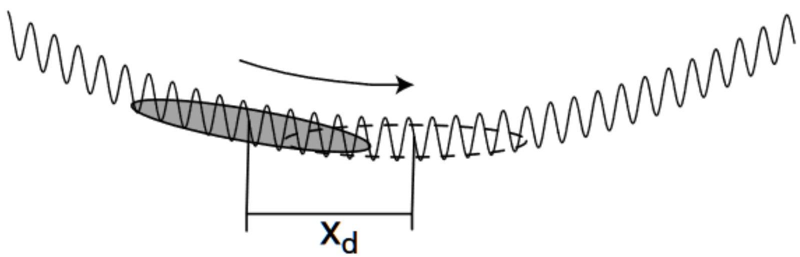

Ott *et. al.*, Phys. Rev. Lett. 92, 160601 (2004).
(Florence)

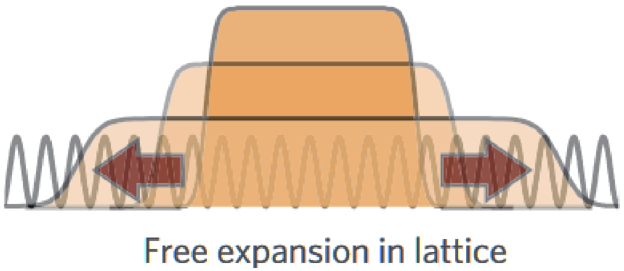

U. Schneider *et. al.*, Nat. Phys. 8, 213 (2012).
(MPQ)

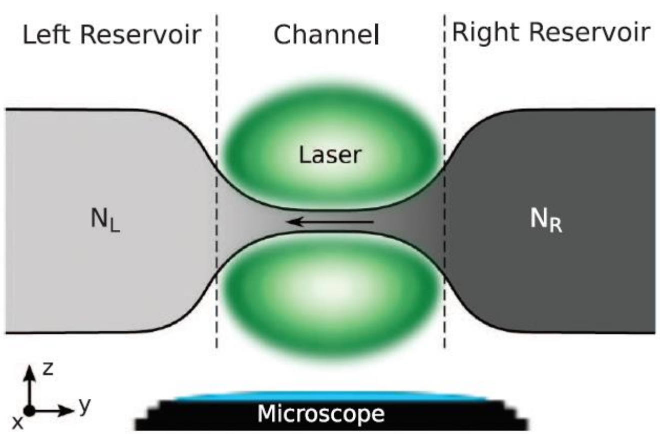

Brantut *et. al.*, Science 337, 1069 (2012).
(ETH Zurich)

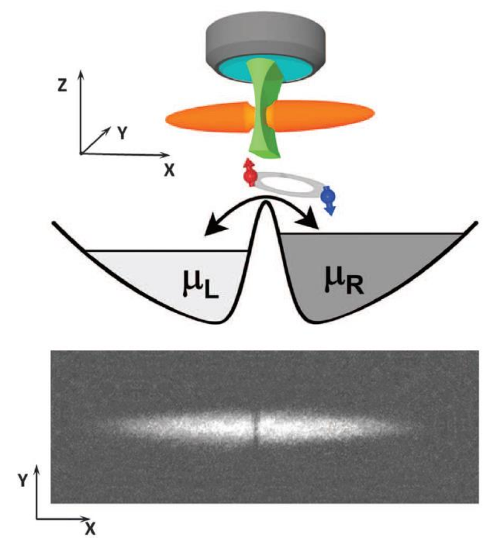

Valtolina *et. al.*, Science 350, 1505 (2015).
(Florence)

Transport in ultracold Fermi gases

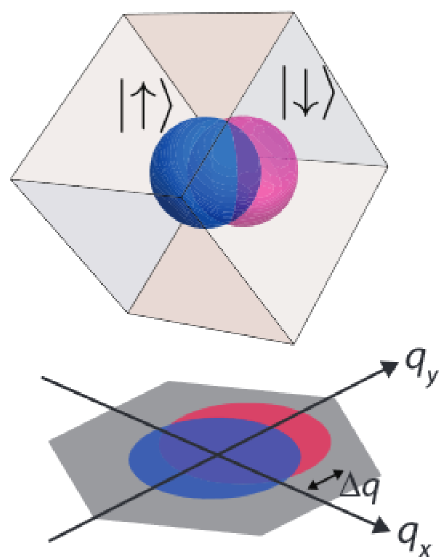

W. Xu, W. McGehee, W. Morong, and B. DeMarco, arXiv:1606.06669 (UIUC)

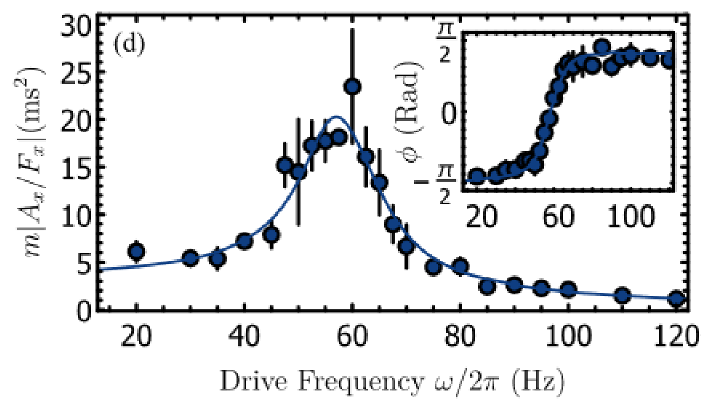

R. Anderson, F. Wang, P. Xu, V. Venu, S. Trotzky, F. Chevy, and J. H. Thywissen, arXiv:1712.09965 (Toronto)

Transport

Conventional (weakly interacting)

Unconventional (strongly correlated)

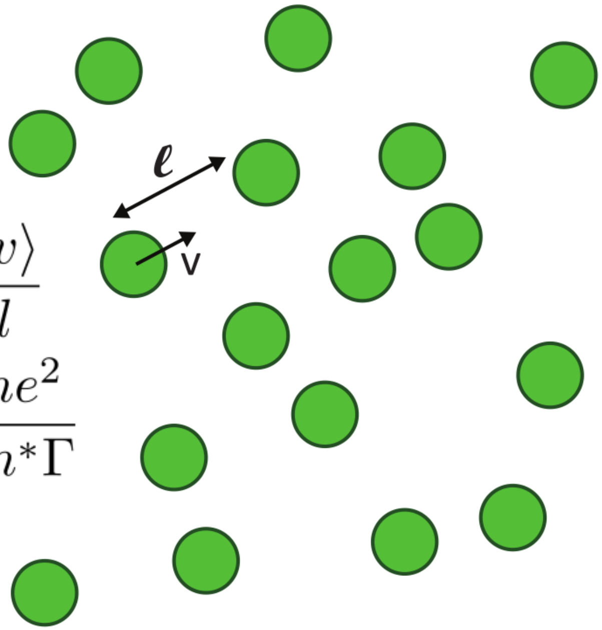

$$\Gamma = \frac{\langle v \rangle}{l}$$

$$\frac{1}{\rho} = \frac{ne^2}{m^* \Gamma}$$

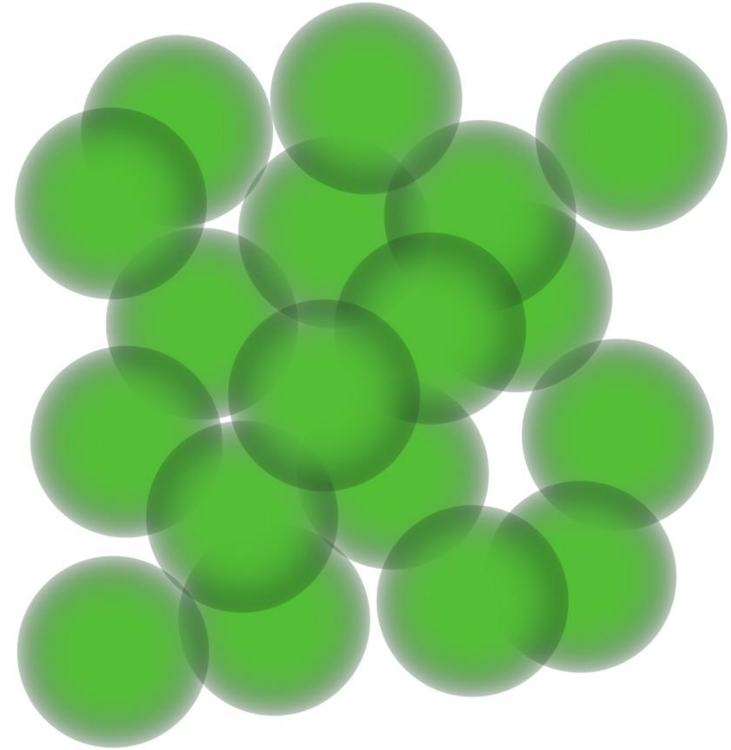

- Charge, spin, energy transported by quasiparticles
- Mean free path must be larger than lattice spacing. Mott-Ioffe-Regel (MIR) limit
- $\rho \sim T^2$, Fermi-liquid

- Strong enough interactions destroy quasiparticles
- Momentum relaxation rate no longer gives resistivity
- “Bad metals” violate MIR limit and commonly show $\rho \sim T$

Bad metals

- No quasi-particle-like transport
  - Violation of Mott-Ioffe-Regel limit
- No Fermi liquid scaling $\rho \sim T^2$ at low temperatures

→ Not explained by conventional theories

Saturation

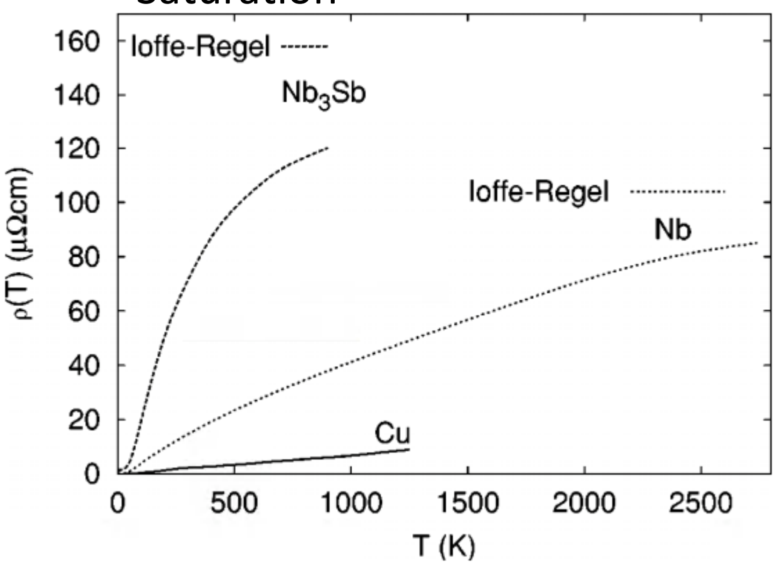

No saturation

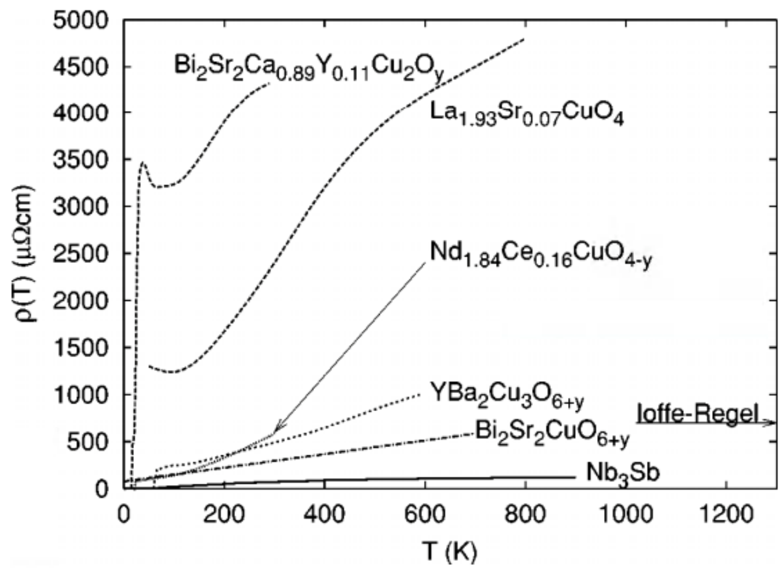

Gunnarsson, M. Calandra, and J. E. Han, Rev Mod Phys 75, 1085 (2003)

Motivation

- Bad metal behavior observed in many condensed matter systems
- But:
  - Hard to measure diffusion in solid state systems
- Here:
  - direct measurement of diffusion possible due to absence of Coulomb interaction

Measuring diffusion

- In long-wavelength limit exponential decay of (sinusoidal) density perturbations
- Diffusion effectively in 1D
- Start with initial sinusoidal density modulation

$$n_k(x,t) = n + \delta n_\uparrow \cos(kx)$$

- $\frac{\partial n_k}{\partial t} = D\Delta n_k = -Dk^2 n_k$ (Fick's law of diffusion)

- $n_k(t) \propto \exp(-Dk^2 t)$

Measurement scheme

Using spatial light modulator

- Real space imaging
- 8x8 mirrors per lattice site
- Single site resolution
  with 650nm light for 752nm lattice
- Fast switching up to few 10 kHz

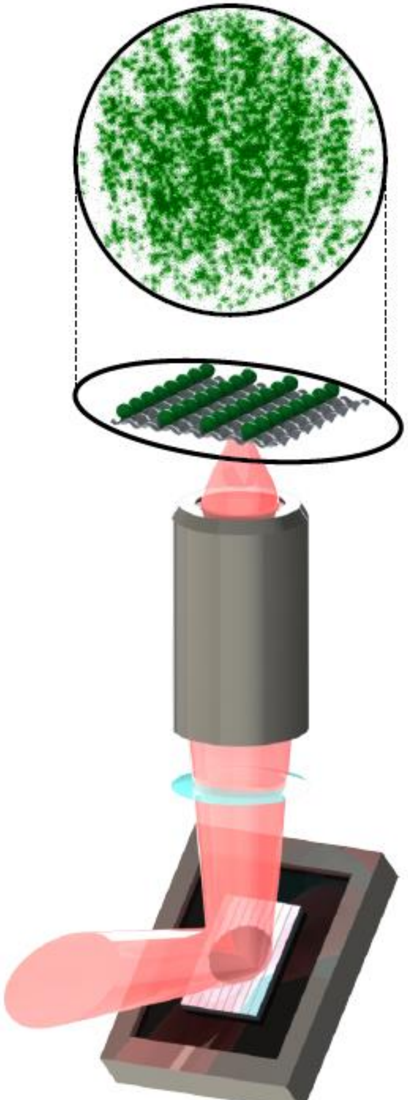

DMD

Binary mirror state

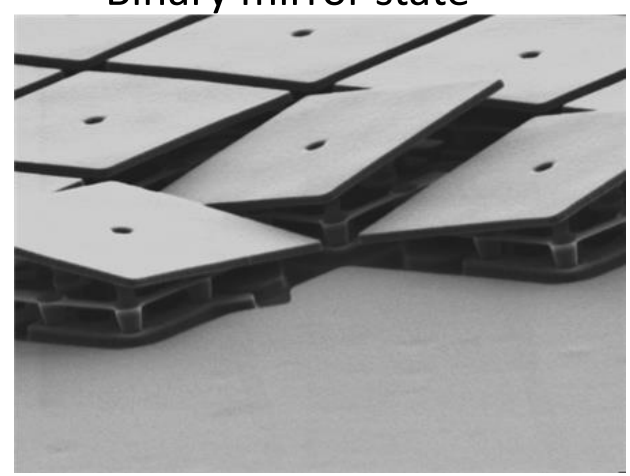

Image by Texas Instruments

Measurement scheme

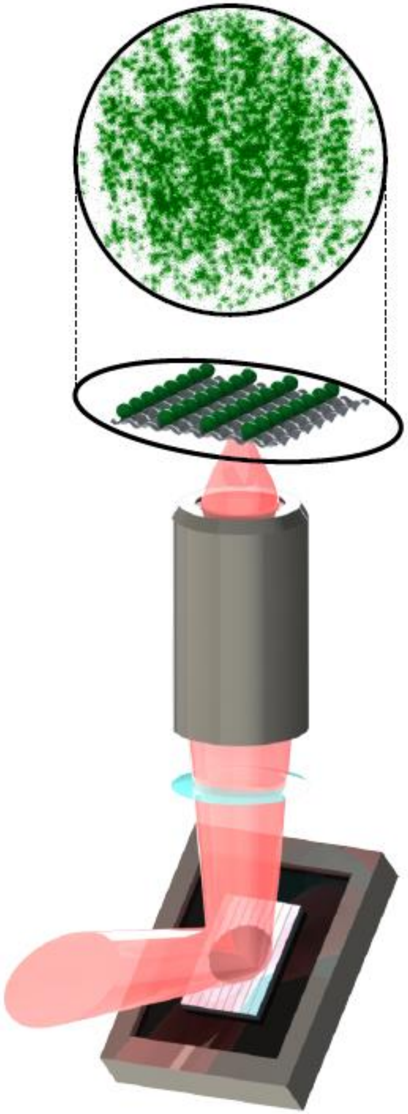

DMD

Using spatial light modulator

- Real space imaging

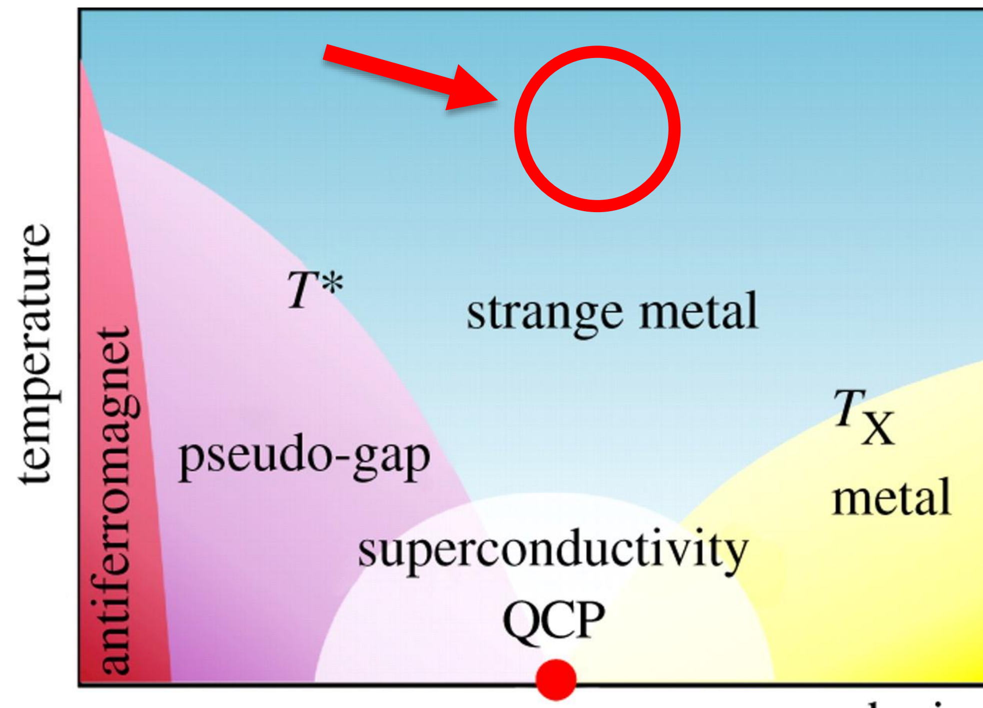

Galanakis et. al., Phil. Trans. R. Soc. A 369 1670 (2011)

Experimental sequence

Imprint density modulation with varying k
and measure decay

U/t = 7.5
n = 0.83

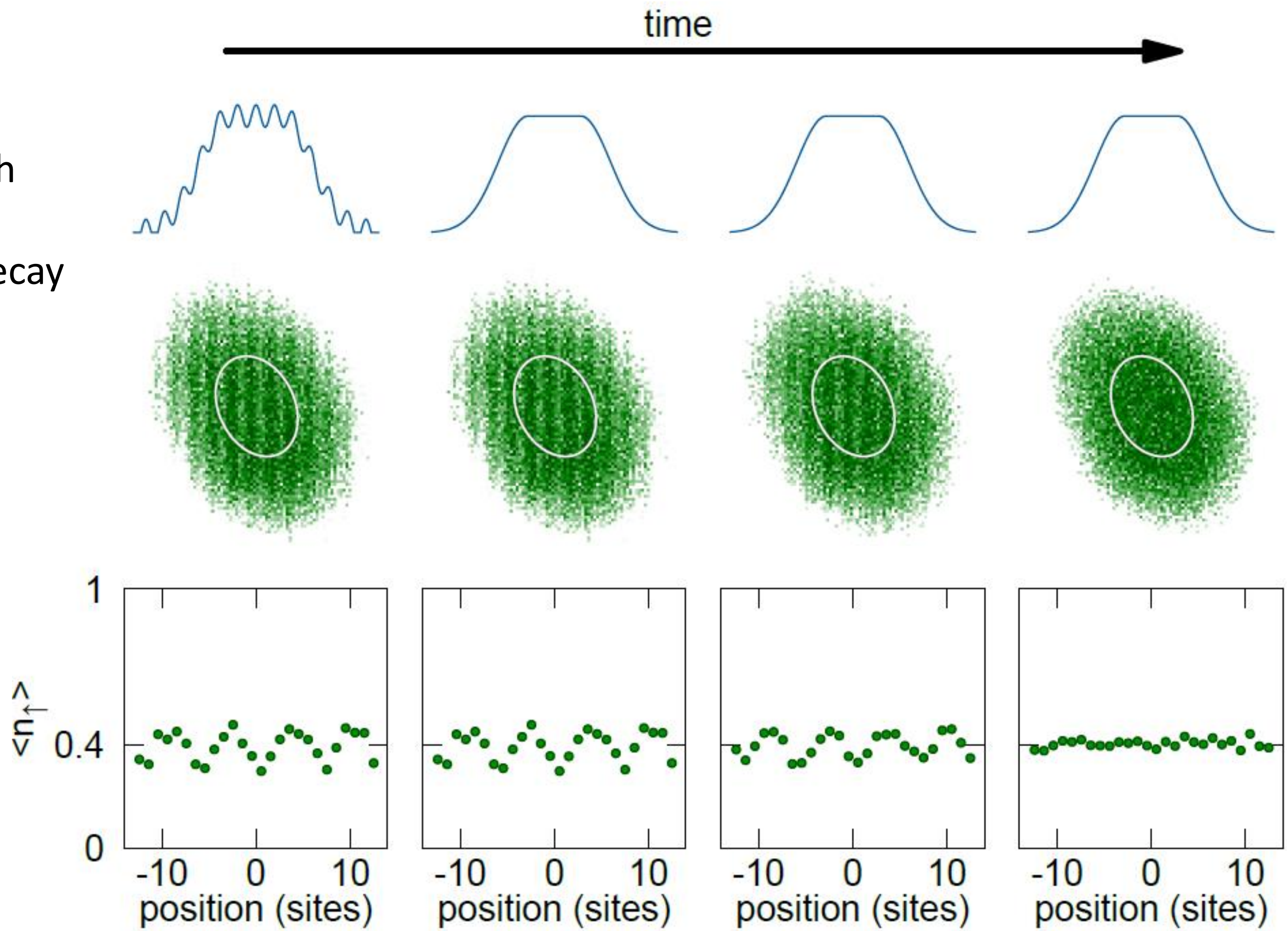

Decaying density modulation

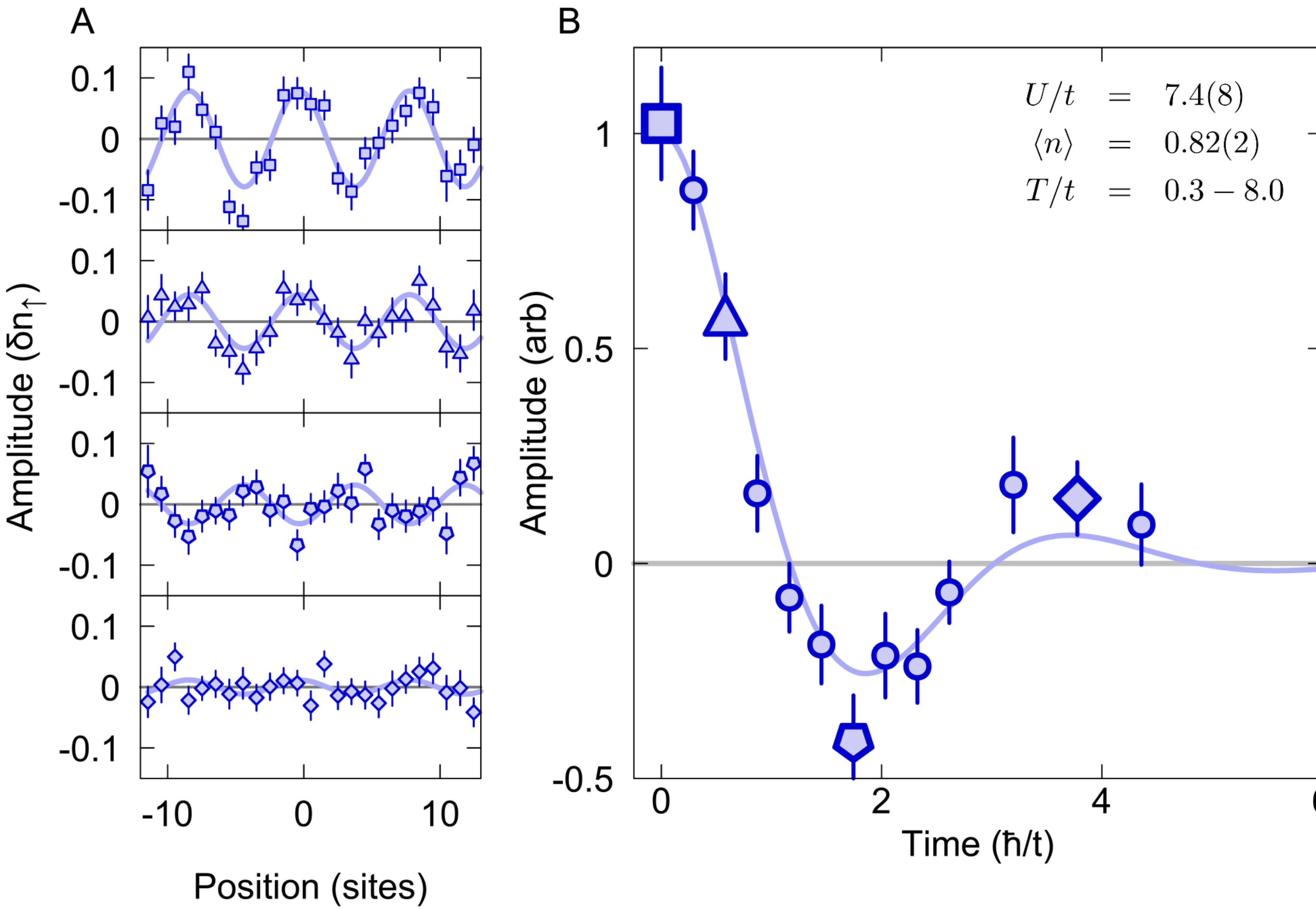

Decaying density modulation

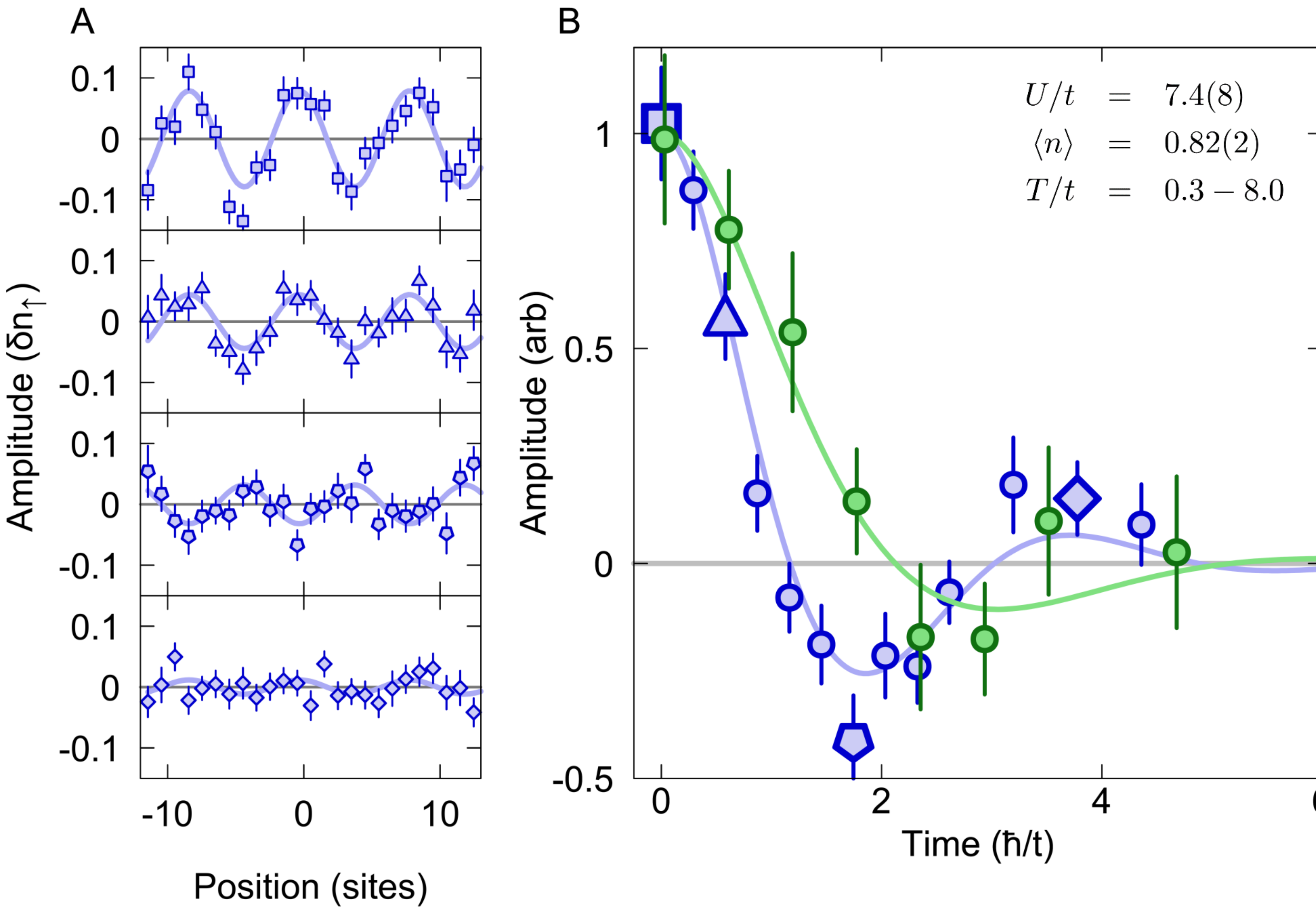

Decaying density modulation

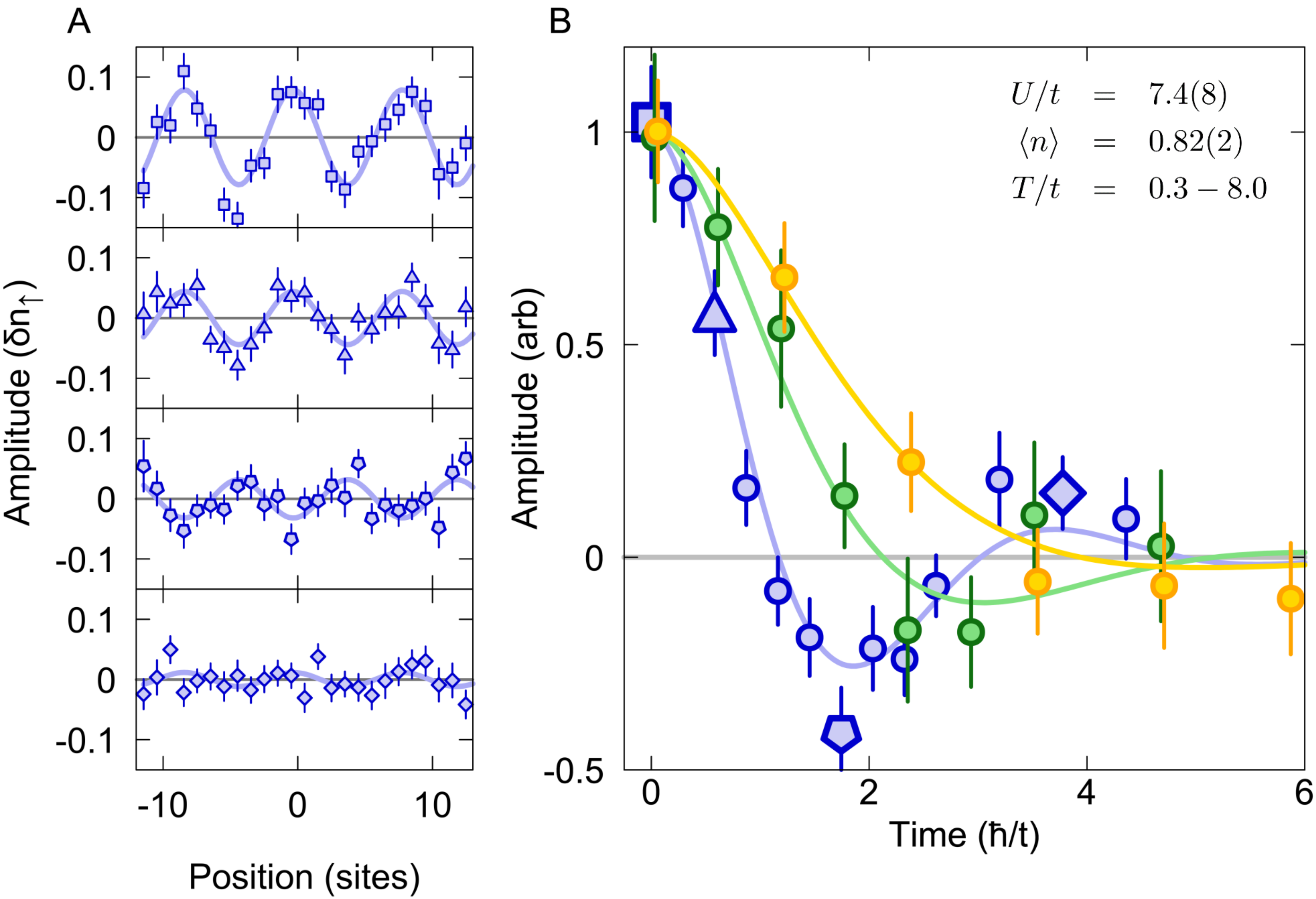

Decaying density modulation

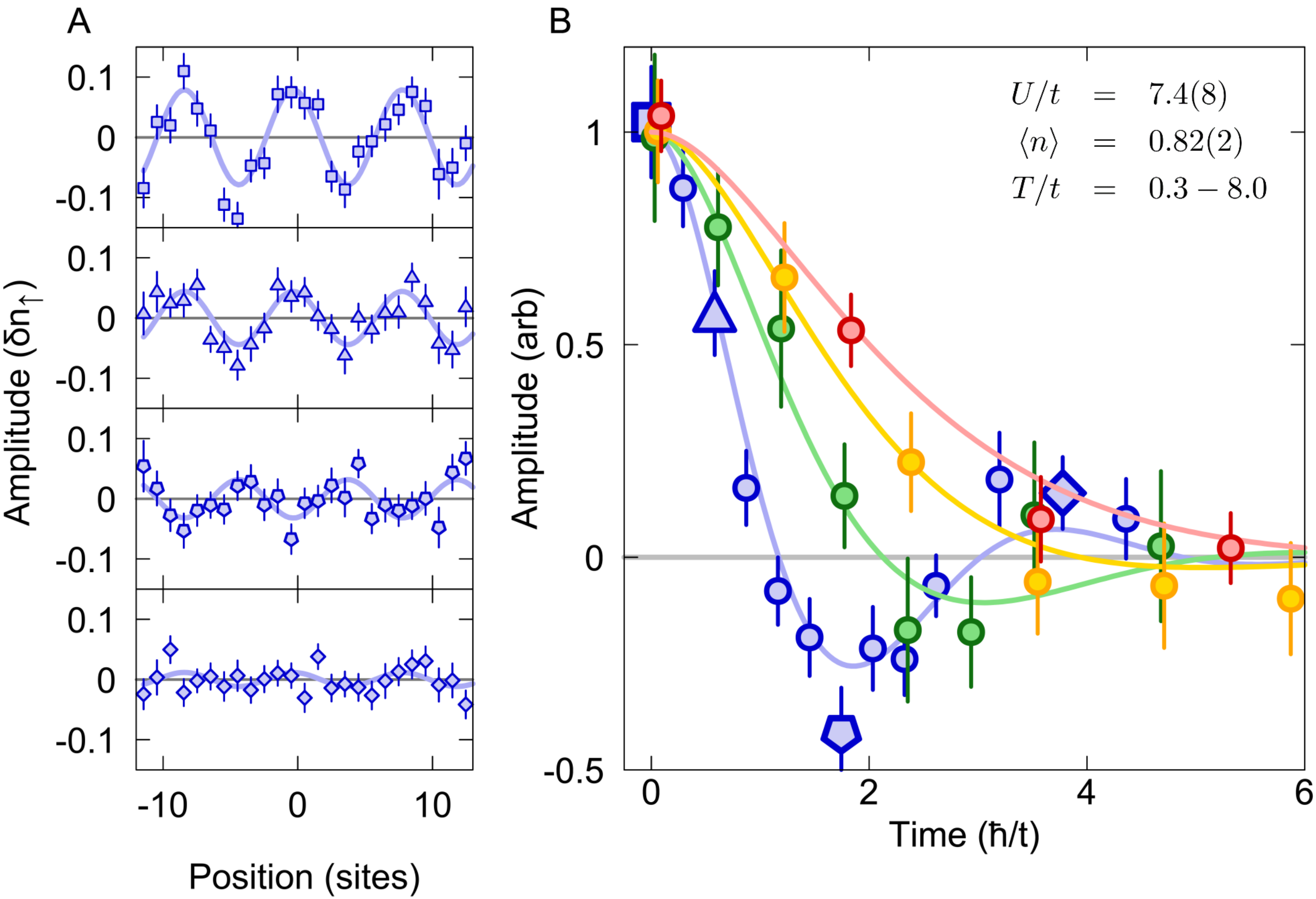

Decaying density modulation

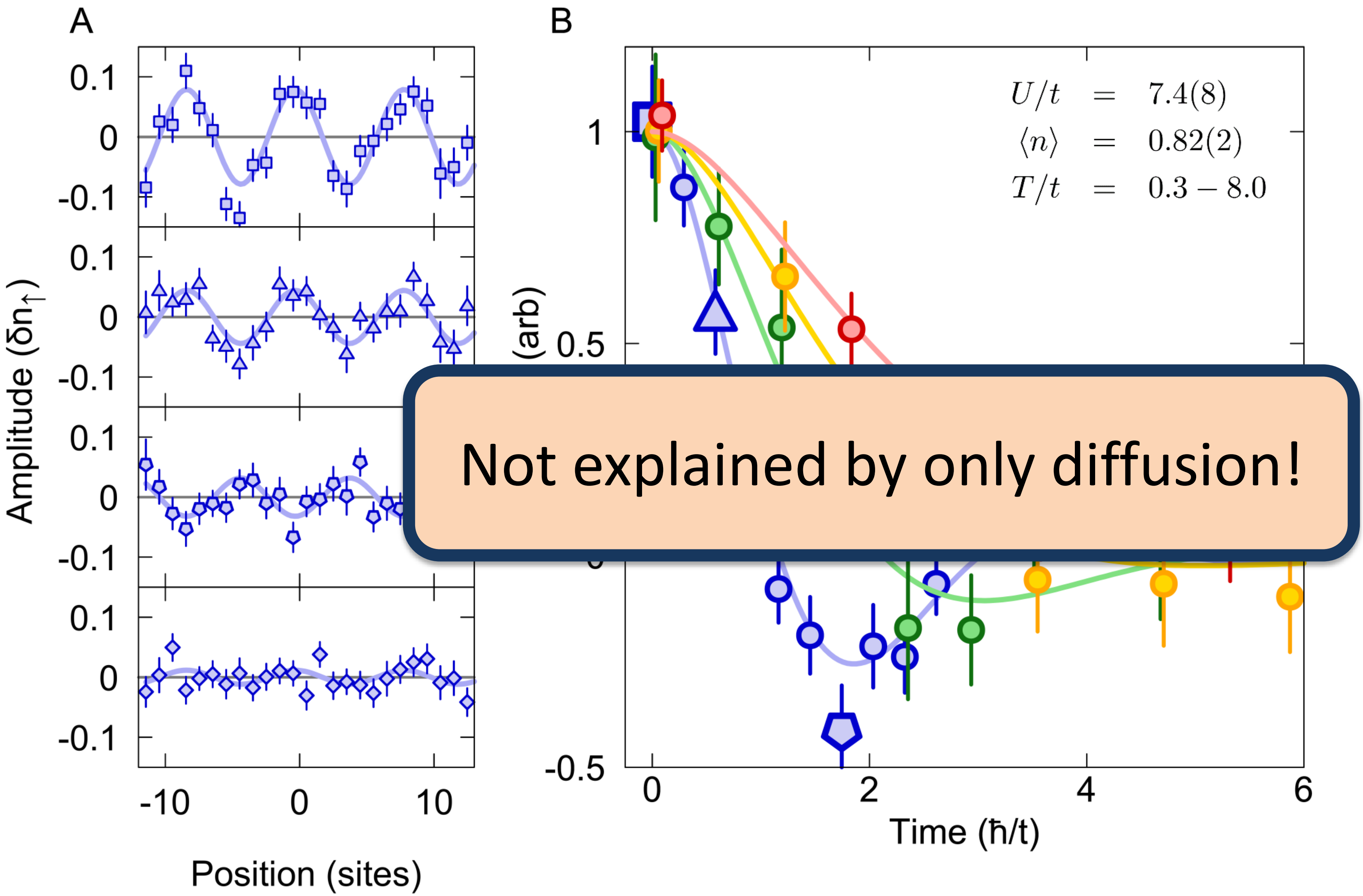

Not explained by only diffusion!

Hydrodynamic model

- Diffusion (Fick's Law) neglects finite time to establish current.
- D, diffusion constant
- Γ, momentum relaxation rate due to *Umklapp* scattering
- Crossover from diffusive mode to sound mode

$$\overbrace{\partial_t n(\mathbf{r},t) \quad = \quad -\nabla \cdot \mathbf{J}(\mathbf{r},t)}^{\text{“charge” conservation}}$$

$$\partial_t \mathbf{J}(\mathbf{r},t) \quad = \quad -\Gamma\,\underbrace{\left(D\nabla n(\mathbf{r},t) + \mathbf{J}(\mathbf{r},t)\right)}_{\text{Fick's Law}}$$

$$\boxed{\partial_t^2 n + \Gamma \partial_t n + \Gamma D k^2 n = 0}$$

Hydrodynamic model fit

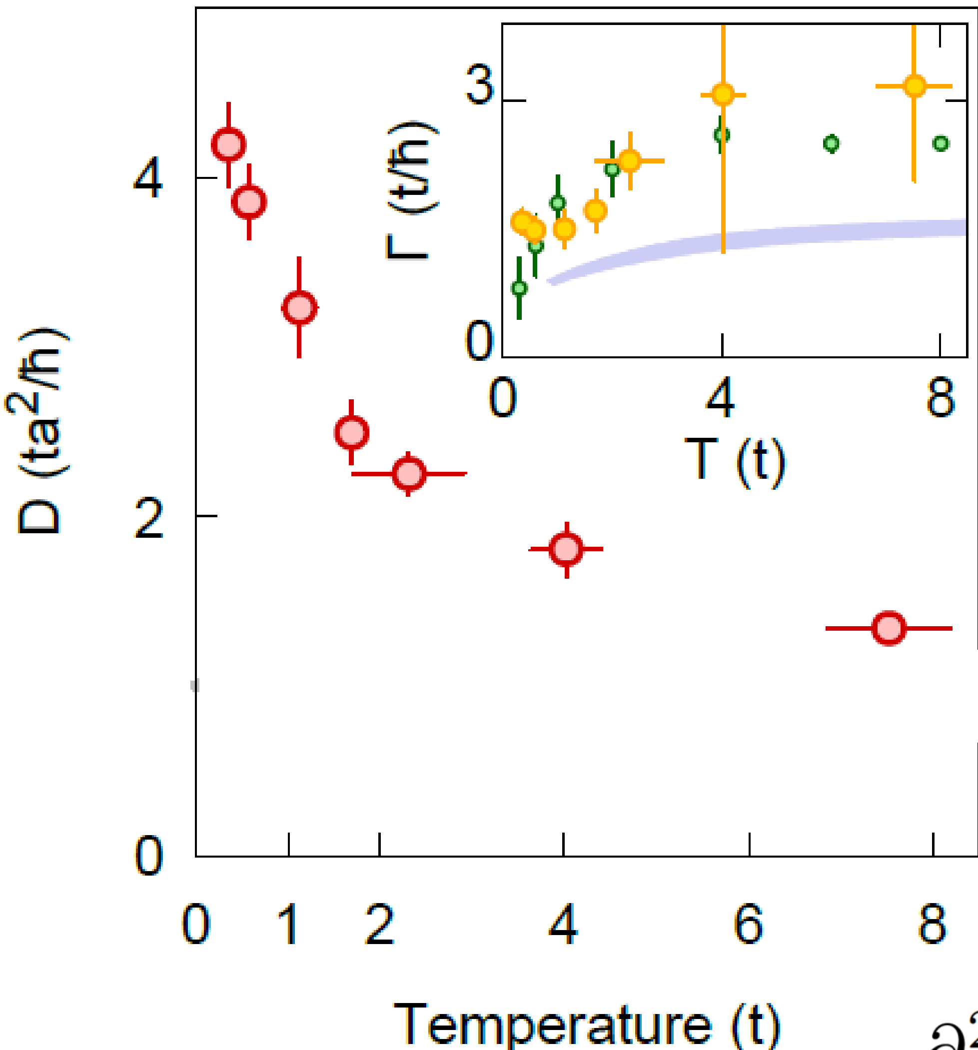

- *Simultaneous* fit of all wavelength data for each temperature
- D saturates at high T, as expected
- Modeling shorter wavelengths requires the momentum relaxation Γ:

$$\partial_t^2 n + \Gamma \partial_t n + \Gamma D k^2 n = 0$$

MIR bound on diffusion

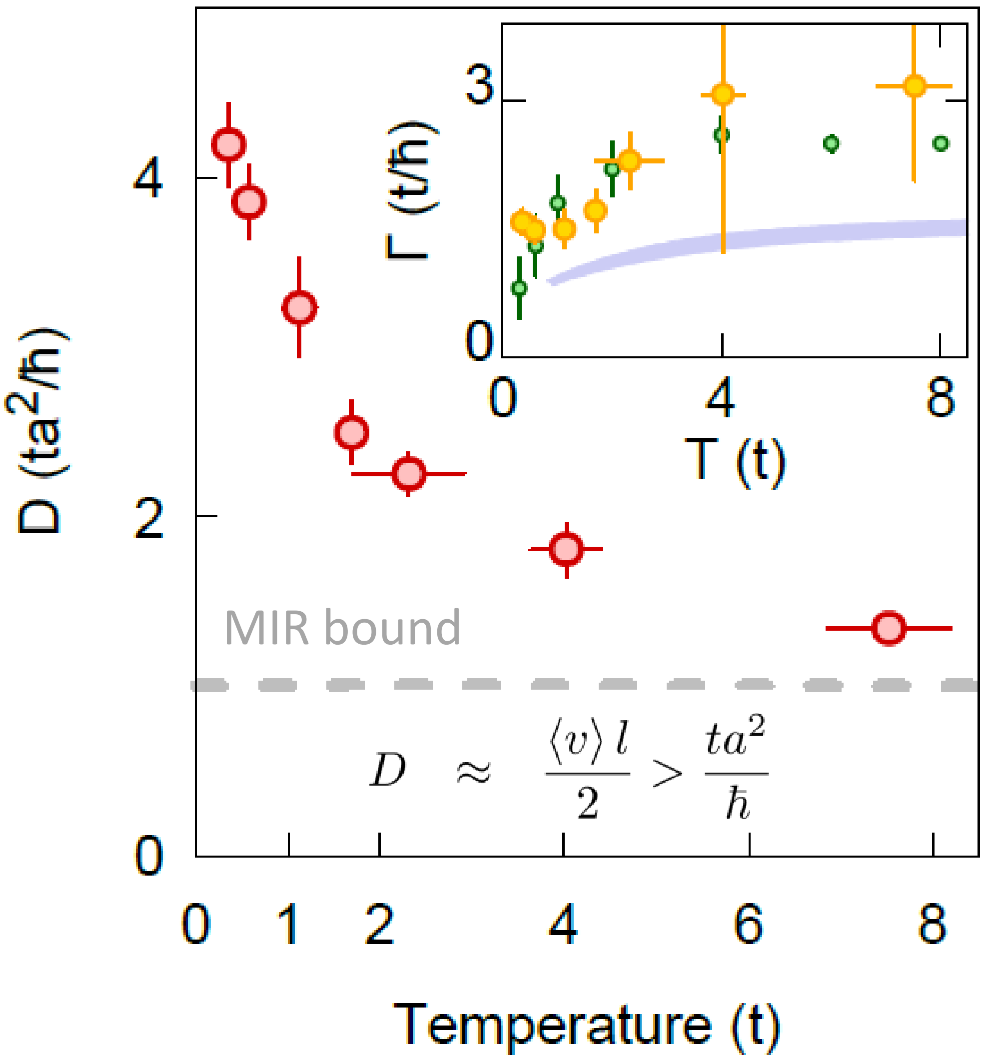

- Mott-Ioffe-Regel bound on diffusion not violated

$$D \gtrsim ta^2/\hbar$$

MIR Bound on Conductivity

- $\sigma = \dfrac{n\hbar}{m^* a^2 \Gamma}\left(\dfrac{e^2}{\hbar}\right)$ (Drude Formula)
- $\sigma \sim \dfrac{nl}{k_f a^2}\left(\dfrac{e^2}{\hbar}\right) > \dfrac{n}{k_f a}\left(\dfrac{e^2}{\hbar}\right)$, ($\Gamma \sim \dfrac{v_f}{l}$ and $l > a$)

$m^* v_F = \hbar k_F$

- Estimate k_f, $\dfrac{\pi {k_f}^2}{V_{bz}} = \dfrac{n}{2} \rightarrow k_f \sim \dfrac{\sqrt{2\pi n}}{a}$
- $\sigma > \sqrt{\dfrac{n}{2\pi}}\left(\dfrac{e^2}{\hbar}\right)$
- Outside of Fermi liquid context, it is not clear how to define k_f or l

Rev. Mod. Phys. **75**, 1085 (2003)
PRB **95**, 041110(R) (2017)

MIR Bound on the Diffusion Constant

- $D \sim \frac{\langle v \rangle l}{2} = \frac{v_f l}{2}$
- Natural units on a lattice are $\left(\frac{ta^2}{\hbar}\right)$, versus (length^2/time).
- $v_f = \frac{2\varepsilon_f}{\hbar k_f} \sim \frac{8ta}{\hbar\sqrt{2\pi}}$, using our previous estimate for $k_f \sim \frac{\sqrt{2\pi n}}{a}$ at half-filling and taking $\varepsilon_f \sim 4t$
- $D > \frac{4}{\sqrt{2\pi}}\left(\frac{ta^2}{\hbar}\right) \sim \left(\frac{ta^2}{\hbar}\right)$ $\qquad l \sim a$

Rev. Mod. Phys. **75**, 1085 (2003)
PRB **95**, 041110(R) (2017)

Temperature Fitting

- Fit singles density and spin up density correlations against total density
- Temperature is the only free parameter

$$
\begin{aligned}
\langle n^s \rangle &= \langle n_\uparrow + n_\downarrow - 2 n_\uparrow n_\downarrow \rangle \\
C^\uparrow(\mathbf{d}) &= 4\left(\langle n_{\mathbf{i}+\mathbf{d},\uparrow} n_{\mathbf{i}\uparrow} \rangle - \langle n_{\mathbf{i}+\mathbf{d},\uparrow} \rangle \langle n_{\mathbf{i}\uparrow} \rangle \right) \\
\mathbf{i} &= (i_x, i_y)
\end{aligned}
$$

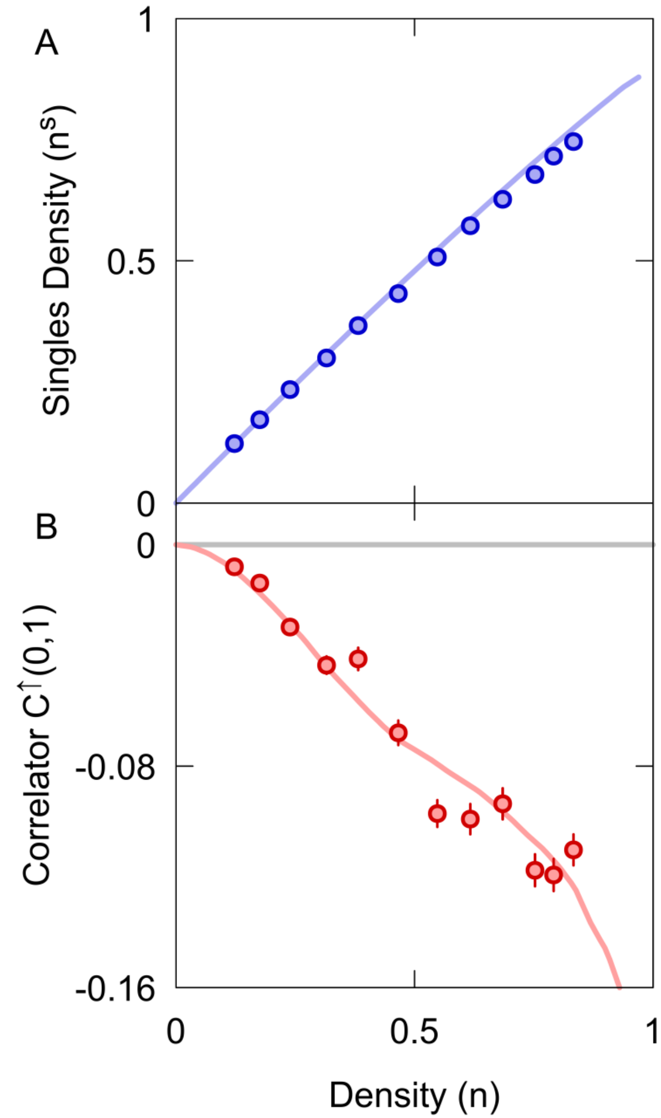

Linear response

- Vary amplitude of initial modulation $\delta n_\uparrow$
- Γ depends on modulation amplitude
- D nearly independent of modulation amplitude

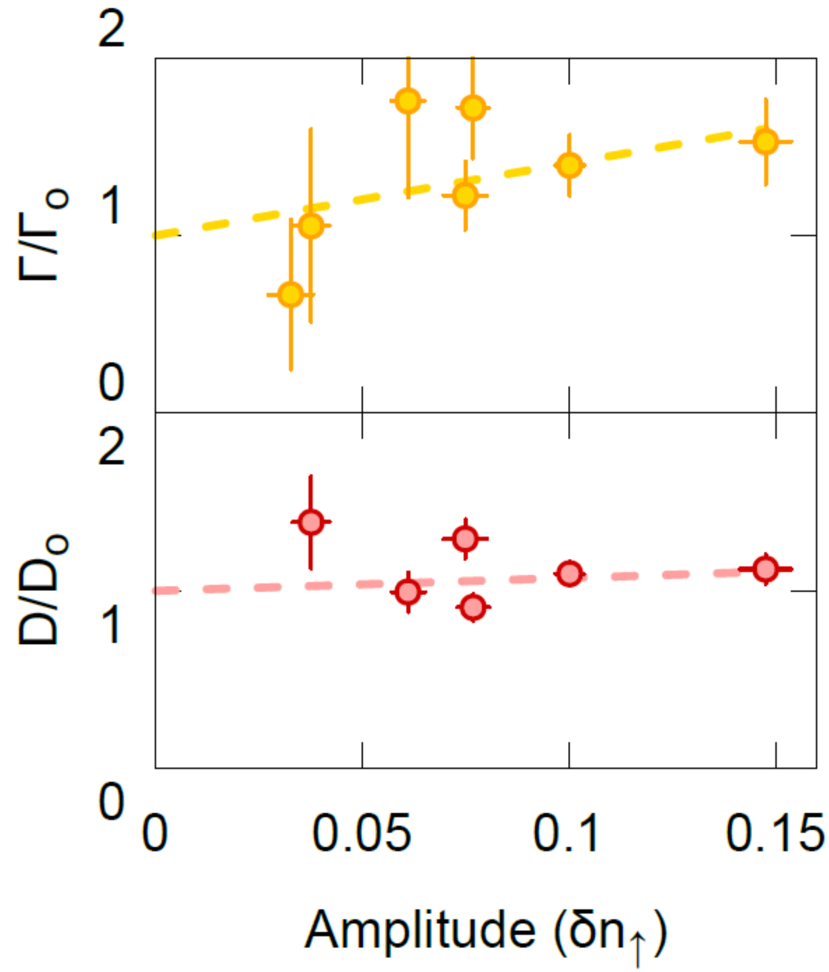

Measurement of resistivity

- Thermoelectric coupling is small
  - Neglect it
- Use Nernst-Einstein relation

$$\frac{1}{\rho} = \chi_C D$$

- Diffusion D from the data shown before
- Compressibility χ_C can be measured independently

$$\chi_c = \left(\frac{\partial n}{\partial \mu}\right)\Big|_T = -\frac{1}{m\omega^2}\left(\frac{1}{r}\frac{\partial n}{\partial r}\right)$$

Compressibility

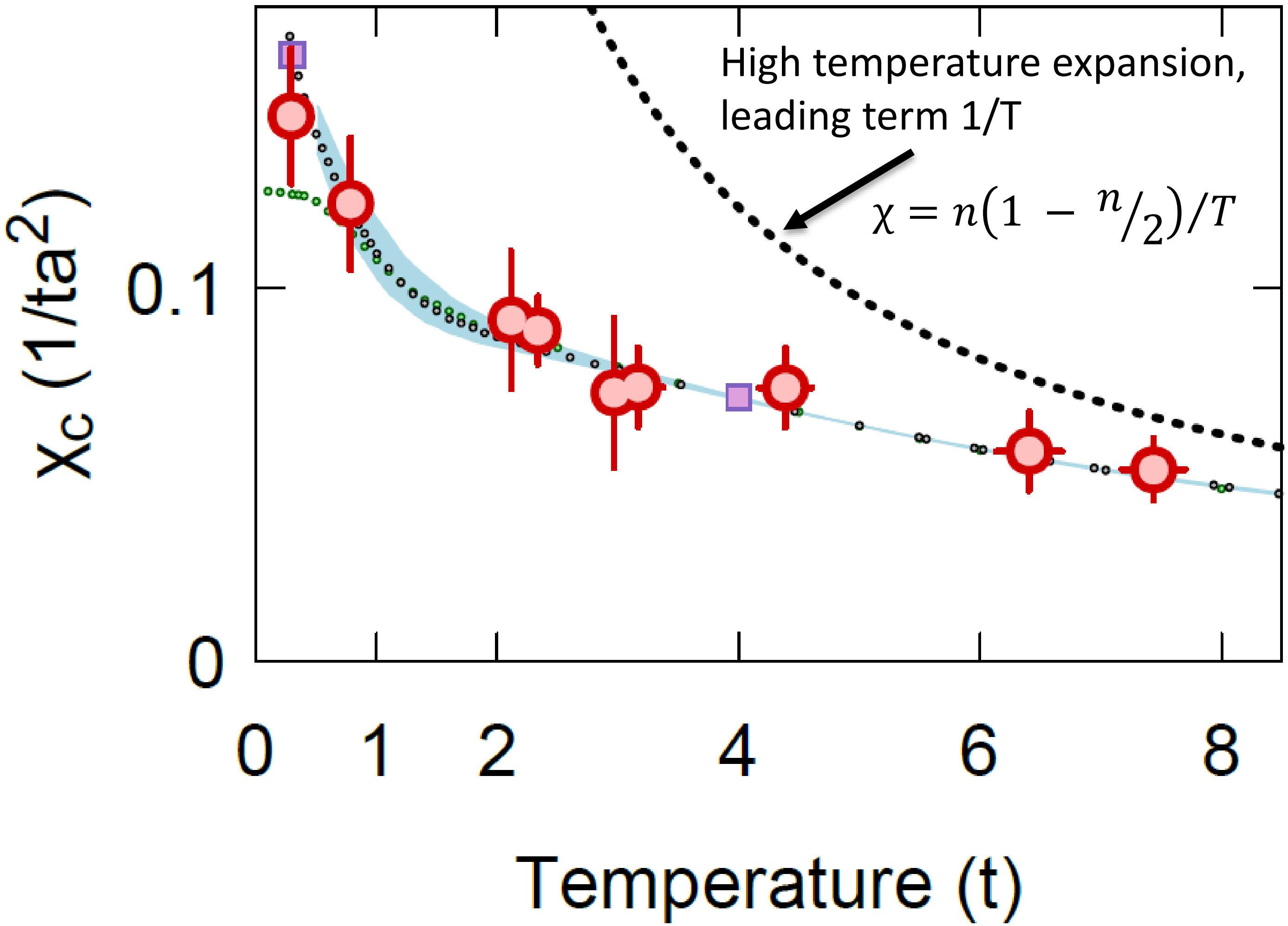

- Good agreement with theory

$$\chi_c = \left(\frac{\partial n}{\partial \mu}\right)\Bigg|_T = -\frac{1}{m\omega^2}\left(\frac{1}{r}\frac{\partial n}{\partial r}\right)$$

Resistivity Versus Temperature

- Resistivity from Nernst-Einstein
  $$1/\rho = \left(\frac{\partial n}{\partial \mu}\right) D$$
- Exceeds resistivity bound inferred from MIR limit ("bad metal")

$$\rho_{\max} \approx \sqrt{\frac{2\pi}{n}}\hbar$$

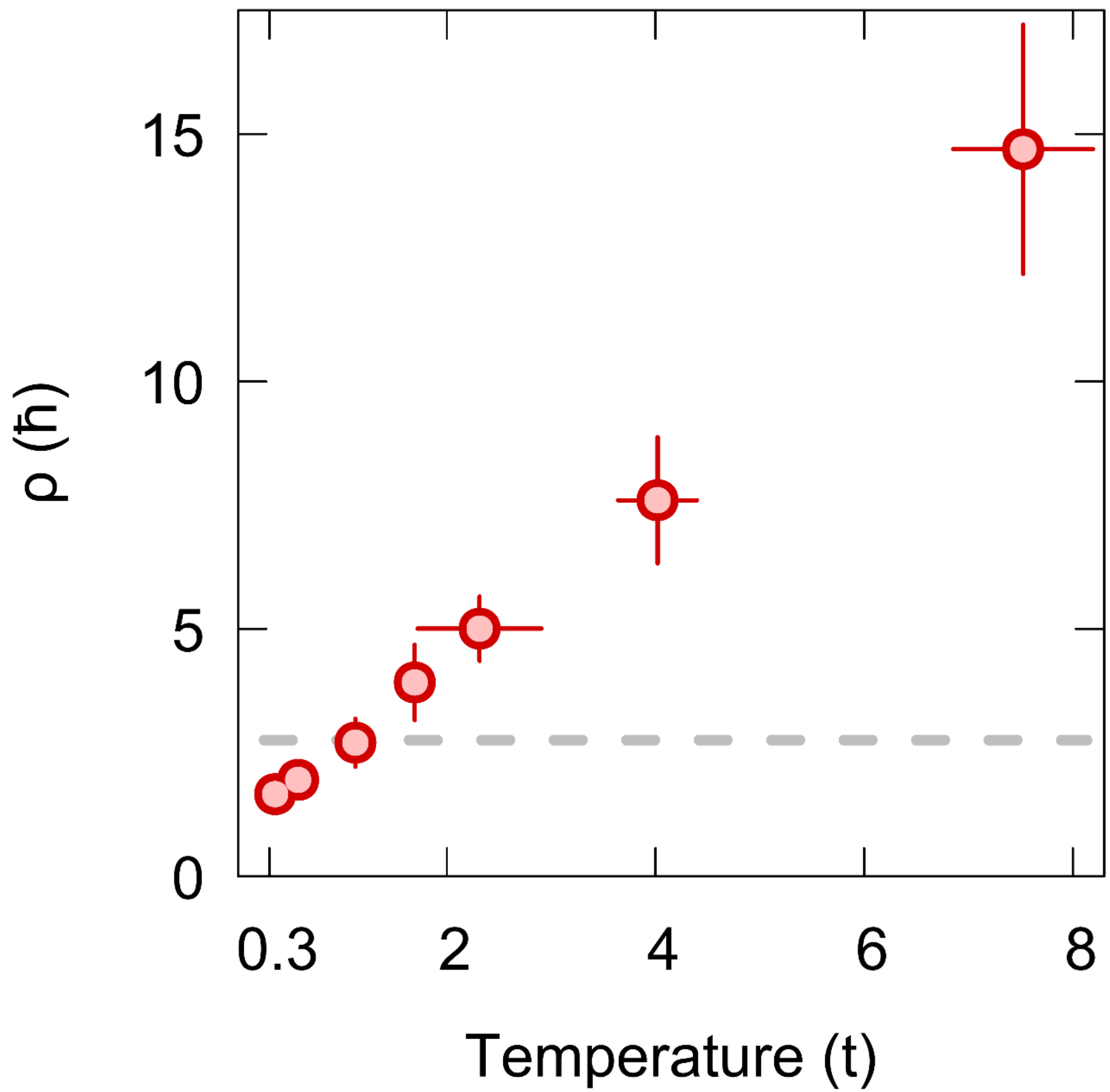

Resistivity Versus Temperature

- Linearity over full temperature range

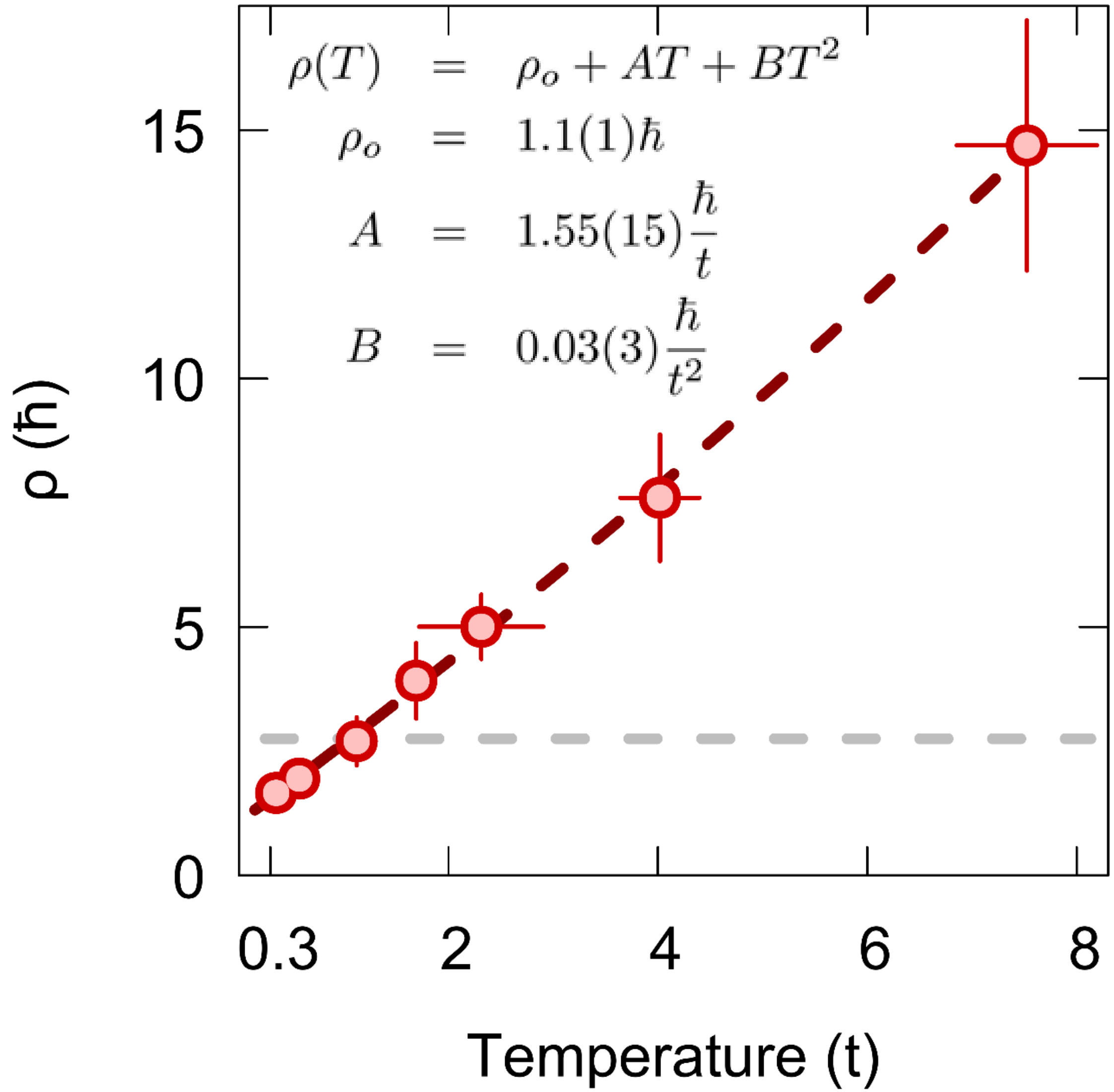

Resistivity Versus Temperature

- Finite-temperature Lanczos on 4x4 reproduces linearity

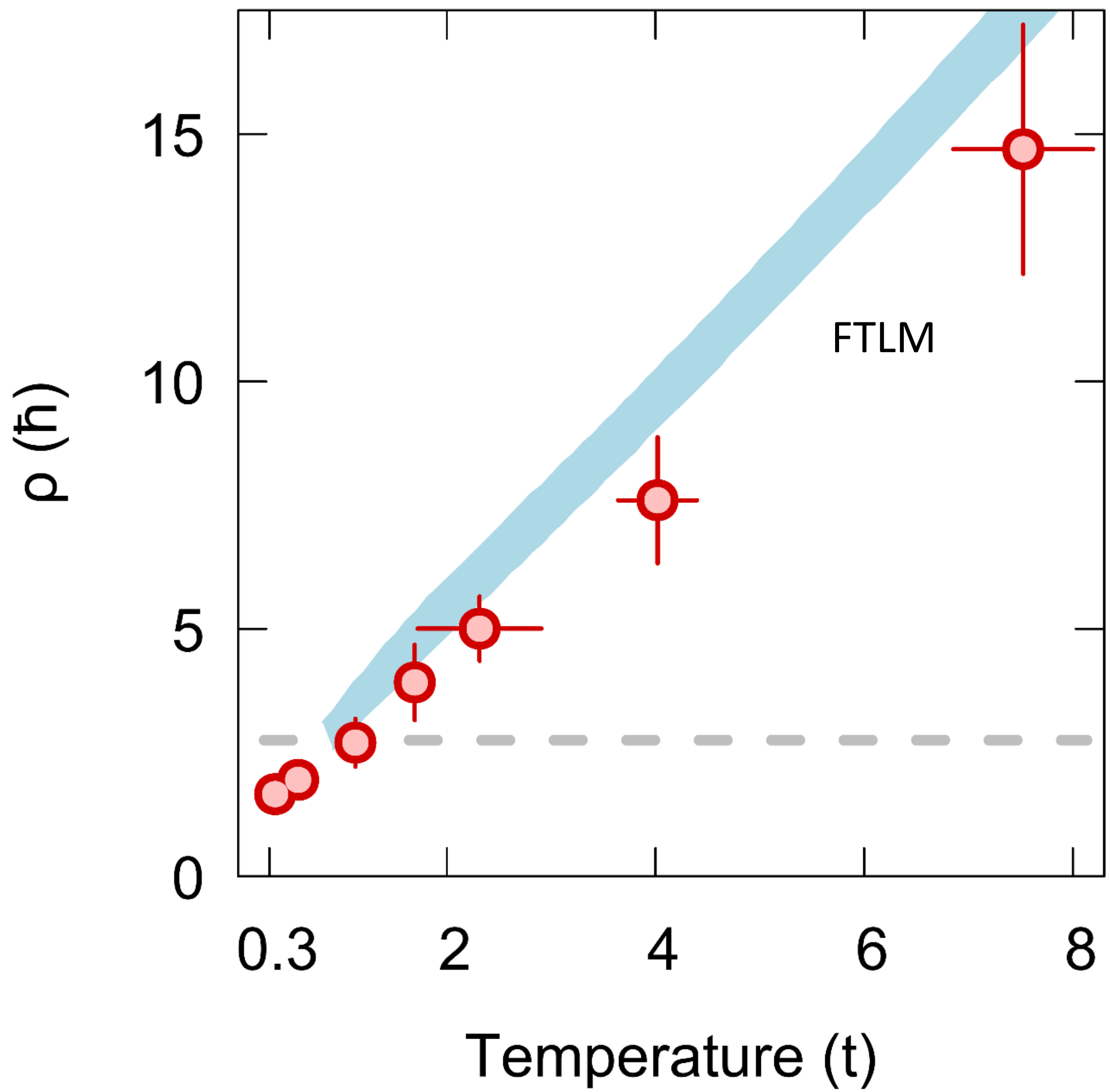

Resistivity Versus Temperature

- Single-site DMFT shows deviations

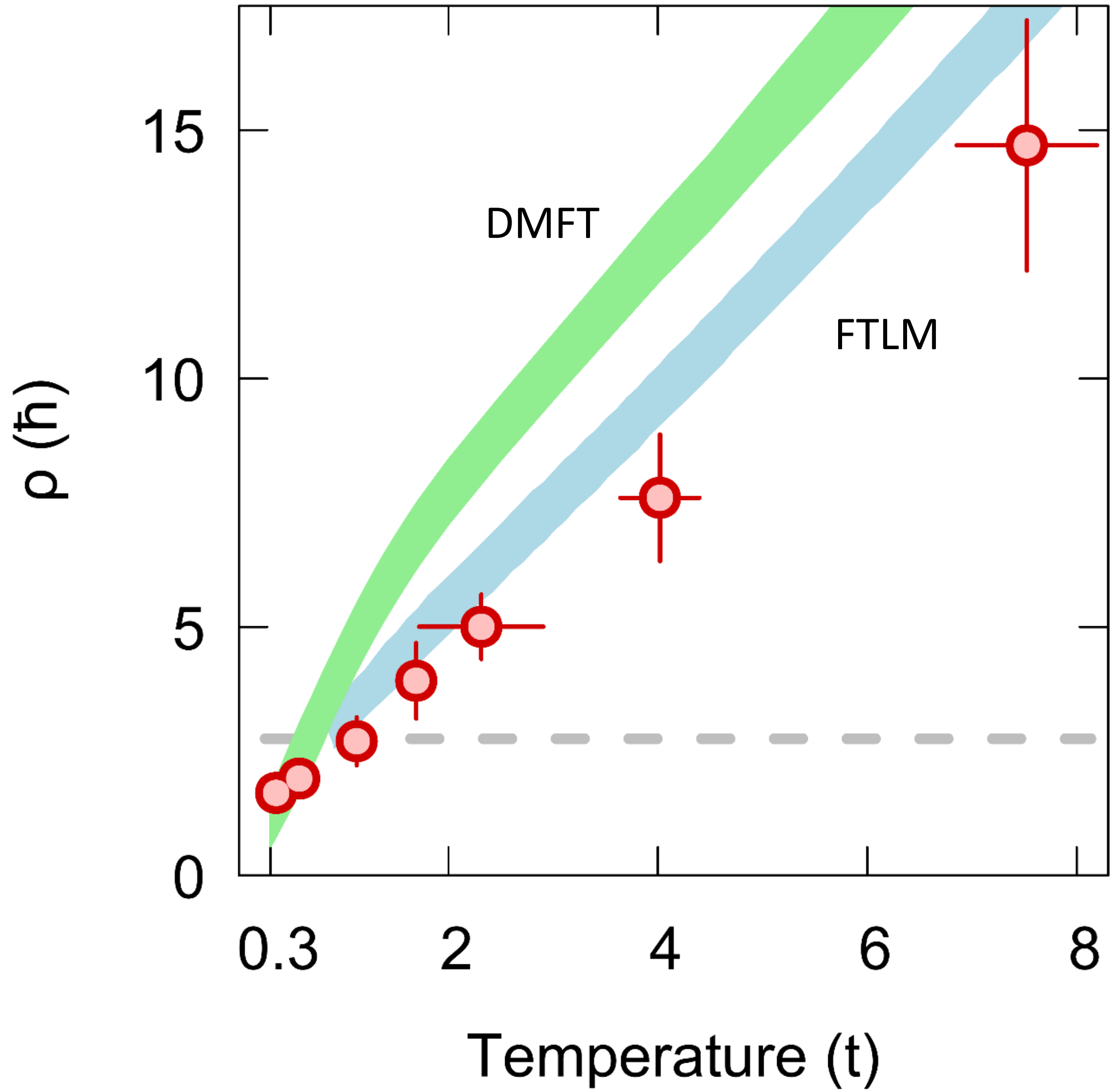

Outlook: Optical conductivity

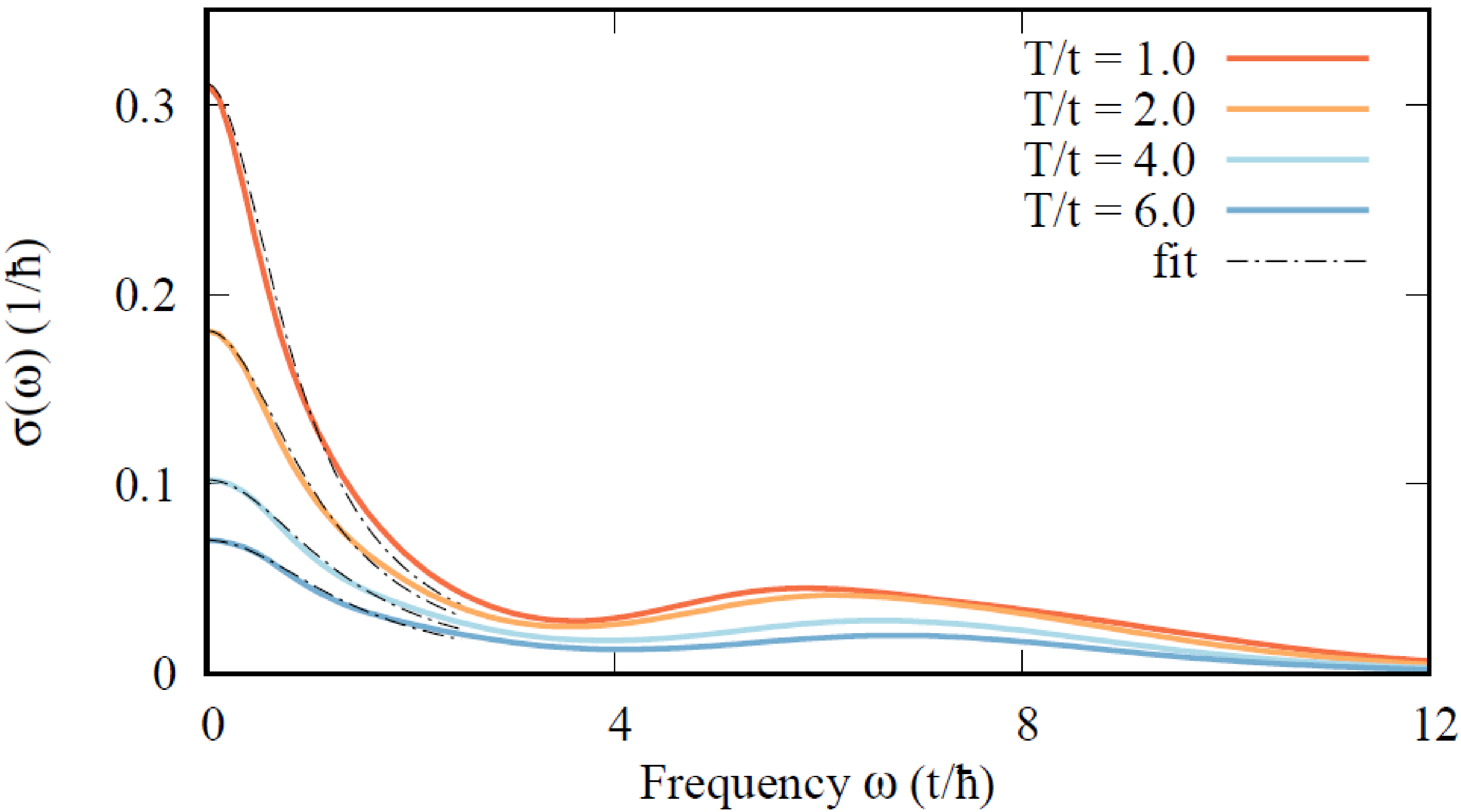

- QMC analytic continuation unstable,
- Finite-temperature Lanzcos good for T/t > 1

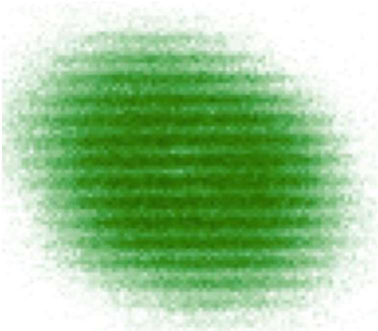

Summary

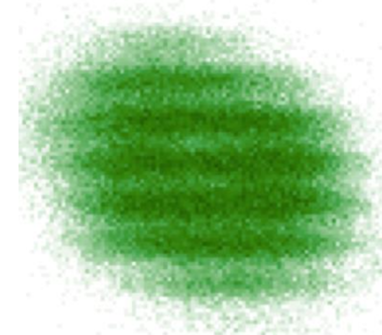

- Observation of T-linear resistivity in a Hubbard system – non-linearities of D and χ cancel
- Violation of resistivity limit caused by temperature dependent compressibility

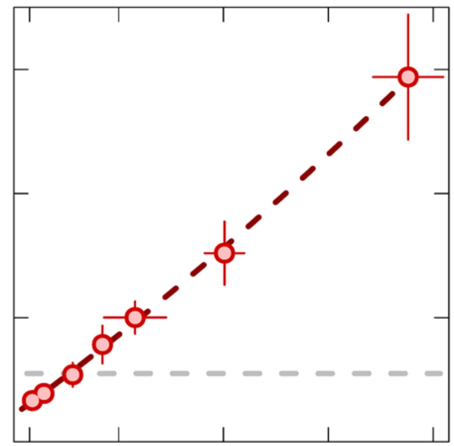

- Exact theory for dynamics (FTLM, DQMC, ...) is extremely challenging at low temperatures. Approximate techniques (DMFT, …) need to be tested. Cluster extensions of DMFT for dynamics remain a challenge.

PI: Waseem Bakr

Peter Schauss

Debayan Mitra

Peter Brown

Elmer Guardado-Sanchez

Theory:

David Huse and Trithep Devakul, Princeton University

Reza Nourafkan, Alexis Reymbaut, Charles-David Hébert, S. Bergeron, A.-M. S. Tremblay, Université de Sherbrooke

Jure Kokalj, University of Ljubljana and Jožef Stefan Institute

Nandini Trivedi, Ohio State University

Thereza Paiva, Universidade Federal do Rio de Janeiro

Ehsan Khatami, San José State University

Funding:

PRINCETON UNIVERSITY

NDSEG

NSF

the David & Lucile Packard FOUNDATION

AIR FORCE OFFICE OF SCIENTIFIC RESEARCH UNITED STATES AIR FORCE

Alfred P. Sloan FOUNDATION

PhD positions available
Starting Fall 2018 – now!
University of Virginia

ps5nw@Virginia.edu